Spring 5-31-2001

Mechanism and kinetics of the reduction of nitric oxide by granular activated carbon induced by PdO/Ai2O3 in the presence of O2

Tian Sang
New Jersey Institute of Technology

Copyright Warning & Restrictions

The copyright law of the United States (Title 17, United States Code) governs the making of photocopies or other reproductions of copyrighted material.

Under certain conditions specified in the law, libraries and archives are authorized to furnish a photocopy or other reproduction. One of these specified conditions is that the photocopy or reproduction is not to be "used for any purpose other than private study, scholarship, or research." If a, user makes a request for, or later uses, a photocopy or reproduction for purposes in excess of "fair use" that user may be liable for copyright infringement,

This institution reserves the right to refuse to accept a copying order if, in its judgment, fulfillment of the order would involve violation of copyright law.

Please Note: The author retains the copyright while the New Jersey Institute of Technology reserves the right to distribute this thesis or dissertation

Printing note: If you do not wish to print this page, then select "Pages from: first page # to: last page #" on the print dialog screen

ABSTRACT

MECHANISM AND KINETICS OF THE REDUCTION OF NITRIC OXIDE BY GRANULAR ACTIVATED CARBON INDUCED BY PdO/Al_2O_3 IN THE PRESENCE OF O_2

by
Tian Sang

NO_x and particulate matter are the main environmental hazards found in Diesel exhaust. In order to explore a novel method to remove NO_x as well as particulate matter, we examined the catalytic reduction of NO_x with solid carbonaceous materials as a surrogate for soot in the presence of oxygen. Pd loaded on Al_2O_3 has been found to be an active catalyst that resists S and H_2O poisoning. A catalyst containing of 2.5% PdO on Al_2O_3 exhibits as high as 90% conversion of NO to N_2 at space velocities of up to 50,000 hr^{-1} and at 500°C.

Most of the experiments were conducted with a feed gas containing 590 ppm NO, 10% oxygen and the balance He as a function of space velocity in the range of 12,000 to 90,000 hr^{-1} and temperature in the range of 350 to 550°C. The result shows that a stable intermediate, CO, is formed by the oxidation of granular activated carbon (GAC) with O_2, and the rate controlling step of the proposed reaction mechanism for the NO reduction is the reaction of NO + CO. Kinetic experiments were carried out in a fixed bed reactor to determine the apparent reaction order and activation energy of the rate determining step. It was found that the activation energy for the rate determine step was 24.1 kcal/mol. The apparent activation energy for the pore diffusion controlled region was 8.97 kcal/mol. Having an apparent activation energy below 10 kcal/mol. indicate that pore diffusion is the likely mechanism in this region.

MECHANISM AND KINETICS OF THE REDUCTION OF NITRIC OXIDE BY GRANULAR ACTIVATED CARBON INDUCED BY PdO/Al_2O_3 IN THE PRESENCE OF O_2

by
Tian Sang

A Thesis
Submitted to the Faculty of
New Jersey Institute of Technology
In Partial Fulfillment of the Requirements for the Degree of
Master of Science in Environmental Sciences

Department of Chemical Engineering,
Chemistry and Environmental Sciences

May 2001

APPROVAL PAGE

MECHANISM AND KINETICS OF THE REDUCTION OF NITRIC OXIDE BY GRANULAR ACTIVATED CARBON INDUCED BY PdO/Al_2O_3 IN THE PRESENCE OF O_2

Tian Sang

Dr. Henry Shaw, Thesis Advisor — Date
Professor of Chemical Engineering, NJIT

Dr. Robert Pfeffer, Committee Member — Date
Distinguished Professor of Chemical Engineering, NJIT

Dr. Richard Trattner, Committee Member — Date
Associate Professor of Chemistry, NJIT

BIOGRAPHICAL SKETCH

Author: Tian Sang

Degree: Master of Sciences

Date: May 2001

Undergraduate and Graduate Education:

- Master of Environmental Sciences,
  New Jersey Institute of Technology, Newark, NJ, 2001

- Bachelor of Engineering in Environmental Engineering,
  Beijing Polytechnic University, Beijing, P. R. China 1994

Major: Environmental Sciences

Presentations and Publications:

Sang T, Shaw H and Pfeffer R,
"Kinetic and mechanism study of reduction of nitric oxide with solid reducing materials by Palladium catalyst,"
The Ninth Annual UNI-TECH Conference at New Jersey Institute of Technology, Newark, New Jersey, April, 2000

This thesis is dedicated to my beloved family

ACKNOWLEDGEMENT

I would like to express my deepest appreciation to Dr. Henry Shaw, Dr. Robert Pfeffer and Dr. Trattner who not only served as my research advisor, providing valuable and countless resources, insight, and intuition, but also gave me support, encouragement, and reassurance.

Special thanks to Dr. Doug Wei for his timely and valuable assistance in the past year. Many of my fellow graduate students in the Otto York building are deserving of recognition for their help and support.

TABLE OF CONTENTS

TABLE OF CONTENTS

(Continued)

LIST OF TABLES

LIST OF FIGURES

Figure **Page**

CHAPTER 1

INTRODUCTION

1.1 Background Information

Vehicular exhaust has been causing serious global environmental and human health problems. The exhaust from gasoline-fueled automobiles operated near stoichiometric air/fuel ratio have been successfully cleaned up by three-way catalytic systems, while the pollution from diesel engines has become much more serious in the last decade. In order to meet anticipated tighter standards for diesel emissions, the development of catalytic aftertreatment systems as well as engine modification are necessary.

The emissions from a diesel engine are composed of three phases: solid, liquid, and gas. The combined solids and liquid emissions are called particulates, or total particulate matter (TPM), and are composed of dry carbon (soot), inorganic oxides, sulfates and organic and inorganic liquids. When diesel fuel is burned, a large fraction of the sulfur present in the diesel fuel is oxidized to sulfate because of the large excess over stoichiometric O_2 present in diesel combustion, the SO_2 and SO_3 react with moisture in the exhaust to become H_2SO_3 and H_2SO_4. The liquid emission are a combination of unburned diesel fuel and lubricating oils, called the soluble organic fractions (SOF) or volatile organic fractions (VOF), which form discrete aerosols with the sulfate, or are adsorbed within the dry carbon particles. The gaseous pollutants include unburned hydrocarbons, carbon monoxide, nitrogen oxides, and sulfur dioxide and are the constituents of the third phase. Diesel emissions are more difficult to treat than those of gasoline engines because they contain a large excess of oxygen, hence, their catalytic treatment is more complicated and requires new technologies.

The popularity of diesel vehicles is derived primarily from their fuel efficiency relative to the gasoline spark-ignited engine. Diesels engines operate very lean, with air-to-fuel ratios greater than about 22. They have good fuel economy, producing less CO_2 per mile driven. It is common for a diesel engine to have a life of 1 million miles, or about 10 times that of a gasoline engine. Power in a diesel engine is archived by compressing diesel fuel and air mixture in order to raise the gas temperature to the point of combustion and drive the piston. As opposed to conventional automotive engines that operate close to stoichiometric, the diesel feed gas mixture operates very lean resulting in a cooler combustion with lower gaseous CO and HC emissions. However, diesel engines produce high concentration of particulates and NOx.

Right now there are several technologies used in aftertreatment of diesel engine exhaust. The first one is diesel oxidation catalysts (DOC). Unlike those of gasoline engines, diesel gaseous HC and CO emissions are relatively low, and their reduction is not necessary to meet the 1994 U.S. truck standards. Thus, the problem is to reduce the particulates, the dry carbon engine emissions can be reduced by engine modification, but this causes an increase in SOF (Heck, Farrauto 1995). One approach to meet emission requirements has been to have the catalyst oxidize the SOF (which represent up to about 65 percent of the particulates), thereby greatly reducing the total particulates emitted. The engine particulate sulfate emissions have been reduced by decreasing the fuel sulfur content from the pre-1994 value of 0.2-0.3 percent to the 1994 value of 0.05 percent. This alone accounts for a drop from 0.05 g/bhp-h to 0.01 g/bhp-h of particulates as sulfate. A combination of reduced fuel sulfur, the presence of a catalyst to reduce the SOF, and engine modification to decrease the dry carbon emitted would bring US trucks into

compliance with standards promulgated for 1994, provided suitable catalysts could be developed (Farrauto, 1996).

The second aftertreatment technology is particulate filters (traps). In the mid-1980's, many engine manufacturers considered using a device to physically filter or trap the particulates on the walls of a monolith. The gases are forced to flow through the monolith wall and exit the adjoining channel. The particulates, having larger particle size than the pore size of the monolith wall were trapped. Since this device had limited capacity before pressure drop become excessive, it is necessary to periodically regenerate it by combusting the soot. The dry carbon particles of the particulates require at least 400-450°C for ignition, and the engine exhaust does not reach such temperatures at all operating conditions. It was hoped that a heterogeneous catalyst would reduce the light-off temperature of the particulates. This approach has met with limited success because the best designs required an expensive and elaborate control system, which is not considered economical for most applications. Only in buses and special off-road vehicles could the expense be justified (Farrauto, 1995). Material development and testing programs, however, are still in progress.

An alternate approach under evaluation is to add certain metallo-organic compounds containing either Cu, Fe, or Ce to the diesel fuel which, when reacted with the trapped particulates, can reduce the temperature for light-off. Because of the potential for emissions of these metal oxides into the atmosphere as fine particulates, it is unlikely that this approach will find broad acceptance. Testing, however, is still proceeding. (Farrauto, 1995)

The most often used technology involves lean NOx catalysts. Given the relatively cooler operating conditions of diesel engines, there will be demand for catalysts to enhance low temperature particulate oxidation to avoid channel plugging under extended idle operation. Furthermore, improved light-off activity for hydrocarbons with minimum use of expensive precious metals will continue to be important for future HC+NOx applications. More active, selective, and durable catalysts will have to be developed to be compatible with improved exhaust system designs. Close coupling of the catalyst to the combustion chamber, hydrocarbon trapping, electrically heated monoliths, particulate traps and so on are under consideration by diesel engine manufacturers to further improve the quality of the diesel exhaust (Farrauto, 1995).

Lean NOx catalysts offer another approach by catalytically reducing NOx with soot and added hydrocarbons to nitrogen. Today's DOCs do not eliminate NOx as do their Otto cycle counterparts. Spark ignition engine use an oxygen sensor to operate near stoichiometric conditions. They oxidize CO and HC and reduce NOx as exhaust oxygen swings between lean and rich operation. Diesels operate lean and have too much excess oxygen in their exhausts, so only oxidation occurs. As now envisioned, a NOx reduction catalyst would foster reactions between NOx and reducing agents in the exhaust, i.e., HC and CO. Some zeolites hold promise here because they are able to capture HC for these reactions. Research must find a way for them to work over the range of temperatures found in diesel engines and with the variety of hydrocarbons present. The creation of lean NOx catalysts must be coupled to engine design so the exhaust has the proper temperature and spectrum of HCs. Another concern that must be addressed is how sensitive these catalysts are to sulfur and water poisoning.

Right now, many research studies are carried out for using alternative fuel in diesel engines. Alternative fuels will grow in importance through the early part of 21st century as a way to control diesel emissions (Heck and Farrauto, 1995). Engines using CNG, LPG, methanol, ethanol, or other fuels may offer the best long-term way to meet exhaust restrictions of emissions because they produce fewer particulates and can be run lean or stoichiometric and so they may be able to meet CO, HC and NOx standards. The initial commercial fuels in this area are now emerging for buses, e.g., CNG and methanol engines are currently being certified by the EPA. Both engines use a DOC to lower HC and CO. However, if alternate fuels are to emerge as a viable alternative, such issues as fuel cost and availability must be overcome.

1.2 Health and Environmental Effects of PM and NOx

Particulate matter (PM) is the general term used for a mixture of solid particles and liquid droplets found in the air. Some particles are large or dark enough to be seen as soot or smoke. Others are so small they can be detected only with an electron microscope. These particles are defined by regulations defining fine particles at less than 2.5 micrometers in diameter and coarser-size particles at larger than 2.5 micrometers. These particles originate from many different stationary and mobile sources as well as from natural sources. Fine particles (PM-2.5) result from fuel combustion from motor vehicles, power generation, and industrial facilities, as well as from residential fireplaces and wood stoves. Coarse particles (PM-10) are generally emitted from sources, such as vehicles traveling on unpaved roads, materials handling, crushing and grinding operations, as well as windblown dust. Some particles are emitted directly from their sources, such as

smokestacks and cars. In other cases, gases such as SO_2, NOx, and VOC interact with other compounds in the air to form fine particles. Their chemical and physical compositions vary depending on location, time of year, and weather.

Respirable PM includes both fine and coarse particles. These particles can accumulate in the respiratory system and are associated with numerous health effects. Exposure to coarse particles is primarily associated with the aggravation of respiratory conditions, such as asthma. Fine particles are most closely associated with such health effects as increased hospital admissions and emergency room visits for heart and lung disease, increased respiratory symptoms and disease, decreased lung function, and even premature death (F. C. Liu, 1996). Sensitive groups that appear to be at greatest risk to such effects include the elderly, individuals with cardiopulmonary disease, such as asthma, and children. In addition to health problems, PM is the major cause of reduced visibility in many parts of the world. Airborne particles also can cause damage to paints and building materials.

In 1997, EPA added two new PM-2.5 standards, set at 15 micrograms per cubic meter ($\mu g/m^3$) and 65 $\mu g/m^3$, respectively, for the annual and 24-hour standards. In addition, the form of the 24-hour standard for PM-10 was changed. EPA is beginning to collect data on PM-2.5 concentrations. Beginning in 2002, based on 3 years of monitor data, EPA will designate areas as nonattainment that do not meet the new PM-2.5 standards.

Nitrogen dioxide (NO_2) is a reddish brown, highly reactive gas that is formed in the ambient air through the oxidation of nitric oxide (NO). Nitrogen oxides (NOx), the term used to describe the sum of NO, NO_2 and other oxides of nitrogen, play a major role in

the formation of tropospheric ozone. The major sources of man-made NOx emissions are high-temperature combustion processes, such as those occurring in automobiles and power plants. Home heaters and gas stoves also produce substantial amounts of NO_2 in indoor settings.

Short-term exposures (e.g., less than 3 hours) to current nitrogen dioxide (NO_2) concentrations may lead to changes in airway responsiveness and lung function in individuals with pre-existing respiratory illnesses and increases in respiratory illnesses in children (5-12 years old) (F. C. Liu, 1996). Long-term exposures to NO_2 may lead to increased susceptibility to respiratory infection and may cause lung alterations. Atmospheric transformation of NOx can lead to the formation of ozone and nitrogen-bearing particles (most notably in some western urban areas) which are associated with adverse health effects.

Nitrogen oxides also contribute to the formation of acid rain. Nitrogen oxides contribute to a wide range of environmental effects, including potential changes in the composition and competition of some species of vegetation in wetland and terrestrial systems, visibility impairment, acidification of freshwater bodies, eutrophication (i.e., explosive algae growth leading to a depletion of oxygen in the water) of estuary and coastal waters (e.g., Chesapeake Bay), and increases in levels of toxins harmful to fish and other aquatic life.

The 1999 National Air Quality: Status and Trend, published by EPA office of Air and Radiation, shows that between 1986 and 1998, national SO_2 concentrations decreased 37 percent and SO_2 emissions decreased 18 percent. Between 1997 and 1998, national SO_2 concentrations decreased 17 percent and SO_2 emissions decreased 13 percent. While

national SO_2 air quality levels have improved, EPA remains concerned about NOx emission control. In the last 10 years, NOx emissions levels have remained relatively constant. Between 1988 and 1997, NOx emissions declined 1 percent, while they increased slightly (by 1 percent) between 1996 and 1997. So, the development of catalytic aftertreatment system of diesel engine for NOx and particulates reduction are very important to improve air quality.

1.3 Palladium Catalysts in Environmental Application

Palladium is a silver-white ductile metal which has a great affinity for hydrocarbon, being able absorb that gas to a greater degree than any other metal. Palladium makes an excellent and versatile catalyst. Its merits have long been appreciated and its uses are constantly increasing in number. Palladium has been shown to have catalytic activity in many types of organic reactions, including hydrogenation, isomerizations, disproportionations, dehydrogenations and oxidations (Bailar Jr., 1973; Wise, 1968; Hartley, 1973). It has been widely used not only in organic chemistry but also in environmental catalysis (Farrauto, et al., 1992).

Most heterogeneous palladium catalysts are manufactured by adsorbing one of two palladium aqueous salts, $Pd(NO_3)_2$ or $PdCl_2$ on a high surface area support. $PdCl_2$ is easily recovered during Pd refining and is less expensive. $Pd(NO_3)_2$ is derived from the chloride, and hence, is more expensive because it must be further processed. However, it is not easy to get rid of the Cl^- ion in preparing palladium catalyst by using $PdCl_2$ as precursor and the presence of chloride is known to have undesirable effects on catalyst performance (Simone, et al., 1991).

Once the catalyst is calcined on a high surface area substrate, the resultant catalyst has a brown color indicative of the presence of a palladium oxide. Unlike platinum, palladium is oxidized to palladium oxide, PdO, in air at temperature above 500°C, and it dissociates to free metal and oxygen at above 875°C (Farrauto, et al., 1992).

The excellence of palladium supported catalyst as a methane oxidation catalyst is well known in the literature. This catalyst is used in the catalytic combustion of natural gas for energy production, produces very little NOx because of the relative low reaction temperature (Mouaddib, et al., 1992). Also, in catalytic oxidation of VOCs for treating industrial gases, it has high activity and good selectivity for the usual automotive pollutants.

The performance of palladium-only three-way catalysts was evaluated by Hepburm, et al. (1994). They showed significantly improved light-off characteristics and greatly enhanced thermal stability compared to currently produced Pt/Rh three way catalyst formulations. In fact, the Pd-only catalysts have better oxygen storage capacity which provide improved CO and NOx conversion capability. Palladium catalyst also have been used in diesel engine, for example, a joint venture between Nippon Shokubai and Degussa is promoting the use of a combination of Pd supported on zirconia with various promoter oxides such as the rare earth for trucks. This technology is in the early stages of commercialization (Farrauto, 1996).

1.4 Literature Review

For diesel emission control, three possibilities, i.e., oxidation, soot trapping and NOx reduction, have been investigated. Oxidation catalysts, mostly precious metal catalysts,

are used to remove CO, gaseous hydrocarbons and SOF, and have already been installed for some diesel-engine vehicles. The development of PM traps has been actively investigated, but problems still remain concerning the reliability of thermal or catalytic regeneration. Since Iwamoto et al. (1990) and Held et al. (1990) independently reported the selective reduction of NOx by hydrocarbons, it has been considered to be the promising process for diesel exhaust aftertreatments. Another option is the simultaneous catalytic removal of NOx and PM, which was proposed by Yoshida et al. (1992) this method can be regarded as a combined process of PM trapping, soot oxidation and NOx reduction by soot, and, if realized, this should be the most desirable aftertreatment of diesel exhausts because it is capable of simultaneously removing both harmful substances.

Table 1.1 summarizes carbon-involving reactions and selected catalysts reported before 1998 for purposes of exhaust treatments. The C-NOx reaction was investigated as a candidate of the NOx reduction process, and catalytic materials were directly supported on carbons. The other two, $C\text{-}O_2$ (soot oxidation) and $C\text{-}NOx\text{-}O_2$ (simultaneous NOx-PM removal) reactions, aim at aftertreatments of diesel exhausts, and the number of publications has rapidly increased the last few years reflecting the increasing concern about the PM emission control. As for catalytic materials, one can easily recognize in Table 1.1 that the elements most frequently used are copper and vanadium as active components and potassium as a promoter.

Tsutsumi et al. (1992) using a rotating fluidized bed to treat diesel engine exhaust gas reported a considerably higher NO conversion over Cu-ZSM-5 catalyst than reported elsewhere in the literature. Conversion of NO at 420°C as high as 95% was reported at

low superficial velocity (15 cm/s), but conversion decreased rapidly to 5% when superficial velocity increased to 55 cm/s. They also found a significant decrease in conversion as the temperature of that gas is decreased to 350°C. The soot removal efficiency was also very high (99%) at a superficial velocity of 18 cm/s, decreasing to about 77-83% at higher gas velocities.

Table 1.1 Catalytic Exhaust Treatments of Carbon

Reactions	Catalyst
C-NO_X reaction	K
	M-La_2O_3-Pt (M = Ni, Co)
	Cs, K, Na
	$Cu_{0.11}H_{0.8}PMo_{12}O_{40}$
	K - M (M = Zn, Cu, Fe, Ni, etc)
	Cu, Fe
C-O_2 reaction	M-La_2O_3-Pt (M = Fe, Co), Cu
	Pt / Al_2O_3
	V_2O_5, V_2O_5 – CuO - Pt
	Cu -V - K
	V_2O_5, $La_2O_3CO_3$
	Cu - (Nb) – K / TiO_2
	Cu-K-Mo- (Cl)
	Various metal oxide
	$PbCl_2$, $CuCl_2$, CuCl
	Fe_2O_3, V_2O_5, Pt
C-NOx-O_2 reaction	Cu/Ce/K
	K/$CuFe_2O_4$
	Cu
	Perovskite-related oxides
	Spinel oxides ($CuFe_2O_4$)

Tsutsumi's (1992) results are very encouraging, especially the much higher conversion of NO over Cu-ZSM-5 catalyst in the presence of soot and oxygen. He pointed out that the mass of soot deposited on the catalyst particles increased to about 50% of the soot throughput after 90 minutes of operation, the mass of soot then started to

decrease with time until it dropped to zero at 200 minutes. This result suggests that the elimination of soot from the catalyst particles must be due to an interaction between NOx, the carbon in the soot and oxygen. An examination of the literature shows that NOx and carbon do react in the presence of O_2 and a catalyst at a temperature as low as 400°C.

The C-NO reaction catalyzed by metal loaded on coal-char both in the presence and in the absence of oxygen was studied by Yamashita et al. (1993) They found that the C-NO reaction was promoted by the presence of oxygen at temperatures as low as 300°C. The ratio of the activity for NOx decomposition to that for carbon combustion in the coexistence of nitric oxide and oxygen depended on the kind of metal catalyst. The order of catalytic activity was Cu>Ca>Ni>none for the C-NO reaction. A high conversion for the C-NO reaction in the presence of oxygen was achieved by copper-loaded brown coal-char. Yamashita, et al investigated the formation of reactive surface intermediate C(O) and stable carbon-oxygen complexes (C-O) by the combination of transient kinetics and temperatures programmed desorption techniques. They also found out that the concentration of reactive C(O) was increased by the presence of both oxygen and Cu catalyst. The enhancing effect of oxygen in the reduction of nitric oxide with chars can be understood in terms of the presence of carbon-oxygen complexes on the char surface. The key feature of the proposed mechanism in this paper of both Cu-catalyzed and uncatalyzed C/NO-O_2 reaction is the enhanced formation of reactive C(O) intermediates, and thus free carbon sites, analogous to that proposed for other carbon gasification reactions. These active sites function either by directly reacting with NO or as acceptors of oxygen species generated on the catalyst surface.

M. J. Illan-Gomez et al. (1995), investigated the NO reduction activity of 10 different carbons and activated carbons, covering a wide range of surface areas and pore size distributions, they found that under the experimental conditions used in the research, all the available surface area of the carbons seems to be effective for the reaction and accessibility problems showing that diffusional limitations are not important. They also investigated some first series transition metals (Cr, Fe, Co, Ni, Cu) as catalysts of the NO reduction by carbon. They found that, at low temperatures iron, cobalt and nickel are the most effective, as they are metals able to chemisorb NO dissociatively. At high temperatures, the activity is larger for cobalt and copper, metals whose oxides are reduced by carbon at a lower temperatures.

D. Panayotov et al. (1996) reported the interaction between NO, CO and O_2 on γ–Al_2O_3 supported copper-manganese oxides. They investigated the activity of γ–Al_2O_3 supported $Cu_xMn_{3-x}O_4$ catalyst towards the reduction of NO with Co at temperature in the range of 150-500°C. They found that the most active catalyst was $Cu_{1.01}Mn_{1..99}O_4$ /γ–Al_2O_3, i.e., the sample where $CuMn_2O_4$ spinel is formed. In the presence of oxygen and the reducing agents CO, oxygen had no blocking effect on the NO+CO reaction.

K. Matsuoka et al. (1996) reported the catalytic reduction of NOx with soot in the presence of oxygen. Pt catalyst loaded on Al_2O_3 coated honeycomb was found to be more active than K, Ca and Cu catalysts. The effects of Pt catalyst and oxygen on the mechanism of C-NO reaction were examined by TPR. NO was completely converted to nitrogen in the isothermal reaction at 500°C, and the high activity of catalyst retained for a long time period. Complete NO conversion was achieved at around 400°C irrespectively of oxygen. NO was mainly converted to nitrogen, but under a certain

condition a small amount of N_2O was produced. Step response experiment revealed that the main nitrogen formation path in the catalyzed C-NO-O_2 system was the reaction between the nitrogen accumulated on carbon and gaseous NO. On the other hand, the coupling of nitrogen on Pt catalyst surface was thought to be the main route for the nitrogen formation for the catalyzed C-NO system without oxygen.

Y. Teraoka et al. (1998) reviewed their studies on simultaneous NOx-soot removal using perovskite-related and spinel-type oxides. Their conclusions are:

(1) Perovskite-related and spinel-type catalysts are superior to simple oxides of transition metals and supported Pt catalyst in the selectivity for NOx reduction into nitrogen, which is defined as a fraction of soot used for the nitrogen formation. This indicates the superiority of mixed metal oxide catalysts.

(2) The peculiar effect of K in promoting the activity and the selectivity is observed in both perovskite-related and spinel-type oxide catalysts. Since it has been reported that K enhanced reactions involving carbons such as gasification, combustion and NO-C reactions, it is speculated that the promotion effect is relevant to the intrinsic nature of K to activate the surface of carbons.

(3) $Cu_{0.95}K_{0.05}FeO_4$ and $La_{0.95}K_{0.05}Cu_{0.95}V_{0.05}O_4$ are the most selective in the present study, but the selectivity to nitrogen formation is as low as about 6%. The enhancement of the selectivity to NOx reduction is required.

(4) Platinum is not a good catalyst for the simultaneous NOx-soot removal, the selectivity to nitrogen formation being low. For example, the addition of Pt to $CuFe_2O_4$ and $Cu_{0.95}K_{0.05}FeO_4$ causes the decrease in the selectivity to nitrogen formation with the activity being almost unchanged.

(5) The partial pressure dependence of the rates of the soot oxidation over $CuFe_2O_4$ catalyst was studied by non-steady state TPR, which is summarized in Table 1.2.

Table 1.2 Apparent Reaction Order of O_2 and NO Partial Pressure for Soot Oxidation over $CuFe_2O_4$ catalysts (Y.Teraoka et al.,1998)

Reaction	Reaction order	Remarks
Soot-O_2	$r(CO_2) \propto P(O_2)^{0.5}$	$P(O_2)$: 0.68-21%, T: 300-400 °C
Soot-NO	$r(CO_2) \propto P(NO)^{1.0\text{-}1.4}$	P(NO): 0.25-1%, T: 360-462 °C
	$r(CO_2) \propto P(O_2)^{0.6}P(NO)^{0.6}$	$P(O_2)$: 1.5-5%, P(NO): 0.225-0.5%
soot-NO-O_2	$r(N_2) \propto P(O_2)^{0.4}P(NO)^{1.0}$	T: 290-342 °C
	$r(N_2O) \propto P(O_2)^{0.4}P(NO)^{1.0}$	T: 359-411 °C

CHAPTER 2

EXPERIMENTAL

Equipment, analytical instrumentation and experimental procedures used in this research are described in this chapter.

2.1 Experimental Apparatus

Figure 2.1 shows the schematic flow diagram of the equipment used in this research. The major components of the system include a quartz tube reactor containing known volumes of catalyst and solid reducing agent, granular activated carbon (GAC). The flow rates of pure gases and mixtures are measured by calibrated rotameters. The reactor system was used to compare catalyst activity and determine catalytic kinetics. The gaseous feed stream was prepared by mixed pure gases and calibrated mixtures before flowing into the reactor. The effluents stream flowed to an analytical train that contains a Furier Transform Infrared Spectroscopy (FTIR) used to measure NO, NO_2, N_2O, CO, CO_2 concentrations and Gas Chromatography (GC) to determine N_2 and O_2 concentrations.

2.2 Equipment and Instrumentation

This section summarizes the design and implementation of experimental equipment and analytical train.

2.2.1 Reactor

The experiments were conducted in a fixed bed reactor using a series of rotameters to blend NO, O_2, He and CO. The reactor was 2.5 cm in diameter by 55cm long quartz tube with a coarse porous quartz disk fused at about two-third of the height of the reactor. The

reactor was placed in a vertical three zone tubular furnace controlled by three independent temperature controllers. The middle zone had a very uniform temperature profile that could be maintained at ± 1°C over the length and diameter of the section. The reactant gas and granular bed materials, containing catalyst and GAC which was placed on the quartz disk were preheated by the furnace. The actual temperature of the bed was monitored with a chromel-alumel thermocouple (type K) which was inserted in the top of the reactor and placed in the center line touching the solids of the packed bed.

Figure 2.1 Schematic Diagram of the Experimental Apparatus

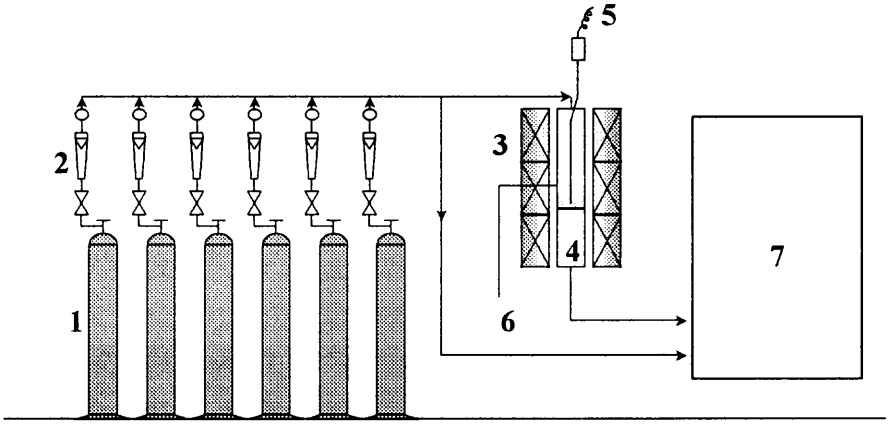

1.Cylinders (He, NO, NO_2, N_2O, CO, CO_2 and O_2)

2. Flow meters 3. 3-zone Furnace 4. Quartz Reactor

5. Thermocouple 6. Temperature Controller

7. Nicolet FTIR G-series 520 and Hewlett Packard 5890A Gas Chromatograph

2.2.2 Gas Chromatography

The GC used in this research is a model HP 5890A with dual detectors consisting of a thermal conductivity detector (TCD) and a flame ionization detector (FID). The TCD is used to measure the concentration of N_2 produced after separation over a 1/8 inch in diameter by 30 feet long stainless steel column packed with 100/120 mesh HayeSep DB. The column was put into an ice bath in order to effectively separate the relatively small N_2 peak from the major O_2 peak using helium as the carrier gas. A relatively large 2.0 cm^3 loop was used in the 6-port gas sampling valve in order to inject a large sample and improve the analysis of N_2.

Table 2.1 Operation Conditions of HP5890A Gas Chromatograph

Detector	TCD, HP5890A	FID, HP 5890A
Detector Temperature, °C	140	300
Injection Temperature, °C	70	350
Column Temperature, °C	0	45
Carrier Gas	Helium	Helium
Loop Volume, cm^3	2	0.02
Packing Materials Mesh Size	100/120 HaySep DR	80/100 Porapak Q
Integrator	HP 3396A	HP 3396A
TCD carrier gas flow rate, cm^3/min	30	30
TCD reference gas flow rate, cm^3/min	50	-
Air flow rate of FID, cm^3/min	-	400
H_2 flow rate of FID, cm^3/min	-	20

CO and CO_2 were separated over 80/100 mesh Poropak Q column and hydrogenated over a nickel hydrogenation catalyst to convert CO and CO_2 to methane and measuring the separate methane peaks with FID. The integration of the

chromatographic peaks was performed with two HP 3396A integrators. Several standard gases containing known concentrations of CO, CO_2 and N_2 in helium were used to calibrate the GC. The operating conditions of the dual column HP5890 GC are listed in Table 2.1.

2.2.3 FTIR

2.2.3.1 Basic Theory of FTIR: The infrared adsorption spectrum of a compound is governed by the absorbance of energy corresponding to the energy transitions in the vibrational and rotational modes of the molecule. Each bond in a molecule has a vibrational frequency which depends on the mass of the two atoms connected by the bond and by the strength of the bond. Therefore, certain frequencies are indicative of certain bonds. Absorbance peaks correlated with the presence of certain functional groups can be found in any reference work on IR.

IR absorption obeys Beer's law and can be used to determine the concentration of the absorbing species. In the infrared region, the common sources are electrically heated elements made of ceramic or alloys. The Nernst glower is composed of rare earth oxides, operates up to about 1800 K, and has a negative coefficient of electrical resistance. This means that the resistance becomes lower as the source is heated, and it may require preheating before a current can be passed at all. The globar is silicon carbide rod, which operates at a lower temperature, about 1600 K, and gives more radiation in the region below $1500cm^{-1}$ than does the Nernst glower. A characteristic of all the IR sources is their generally low output of radiation. The inherent sensitivity of IR spectroscopy is low, due to the limitation of the energy available from the source and the low sensitivity of the

IR detectors. Therefore, a design using a Michaelson interferometer instead of a monochromator is often used. This is the basis of Fourier transform infrared.

In the infrared region, the interferometer replaces the grating monochrometer for use in spectrophotometry. Instead of spreading the spectrum in space as a grating does, the interferometer measures all the frequencies simultaneously. This gives a major advantage in sensitivity since all the radiation is observed at all times. Light from the source is passed through a beam splitter. Half of the incident radiation is reflected onto a moving mirror, and the rest onto a stationary mirror. The beams reflected from the two mirrors are recombined at the beam splitter. Depending on the difference in distance between the paths followed by the two beams, some wavelengths are constructively interfered and the rest are destroyed. The distance changes smoothly as the mirror moves, so that each wavelength is modulated in a sine wave pattern. The entire spectrum is the composite of these single waves, each of a different frequency. The sine wave frequency is related to the frequency of the original wave, but is much lower, so the detector can follow it. The frequencies of the sine waves (f) falling on the detector are functions of the velocity of the moving mirror (v) and the wavelengths of the incident radiation (λ).

The detector signal is sampled at precise intervals as the mirror moves. The moving mirror is the heart of the instrument, and the mechanism that moves it must be stable and reproducible. A helium/neon laser is used to calibrate the alignment, monitor the mirror scan rate, and for a wavelength comparison standard. The complex interferogram produced by the detector is changed if some of the frequencies are absorbed by the sample. Therefore, it contains all the information of a standard spectrum. The interferogram is deconvoluted by computer, using a mathematical function known as

Fourier transformation, and the original spectrum is reconstructed. Because the wavelength of the incident radiation is involved in the equation, it can be seen that the interferometer is not practical for use at shorter wavelengths in the visible or UV. An interferometer to be used at short wavelengths would require mechanical tolerances for the mirror movement and alignment which would be impractical for ordinary use.

The Fourier transform infrared spectrometer depends heavily upon computer power to deconvolute the inteferogram and reconstruct it into a spectrum. As computers have become more powerful and inexpensive, the cost difference between the FTIR and the grating IR instrument has steadily diminished. Since the FTIR can report an IR spectrum in a few seconds, compared to several minutes for a grating instrument, the small additional cost for the FTIR is usually justified.

There are additional advantages to FTIR. Each scan takes only seconds to perform and the entire spectrum exists in digital form in the computer. Therefore, it can easily and rapidly do many scans of a sample and to average these, greatly improving the signal to noise ratio. Sensitivity is better because there are no slits to remove parts of the incident radiation and reduce radiant throughput. Resolution is also better than in comparable grating instruments. Finally, because the entire spectrum is produced in digital form in the computer, subsequent calculations are easily done. Backgrounds can be subtracted, and a spectrum can be compared to thousands of standard spectra in a computer library, with a few keystrokes.

Because of the low power of IR sources, gaseous samples, being of low concentration, need a longer path length. Gases can be placed in a cylindrical cell with IR transparent windows at the ends. The cells have inlets and outlets so that they can be

purged with the sample gas. The windows are cut from a KBr crystal or other crystals that are chemically compatible with gas stream being measured. The pressure of the gas sample can be varied. Highly absorbing samples can be measured at pressures of a few millimeters of pressure, while low concentration samples can be used at higher pressures. For trace level samples, the required path length may be so long that the cell would be impossible bulky. These are aligned so that the incoming beam of radiation is bounced back and forth through the sample several times before being brought to the exit slit. The adjustment and alignment of these cells are usually carried out using a visible laser beam.

Mathematical models involving the specific absorbances of compounds at different wavelengths are being used to develop algorithms to find the signature of specific component in the mixture. This is possible in IR spectroscopy because of the information richness of the spectra.

2.2.3.2 FTIR Operating Parameters :

FTIR Nicolet 520

Instrument:

Detector: DTGS KBr

Beam splitter: KBr

Source: IR

Spectral range: 4000 – 400 cm^{-1}

Gain: 3

Aperture: 100.0 cm^{-1}

Mirror velocity: 1.5825

Data Collection:

No. of sample scans: 20

No. of background scans: 32

Resolution: 1

2.2.3.3 Calibration: The five components studied under the experimental condition and their concentration ranges are listed in Table 2.2.

Table 2.2 Range of Concentrations Studied

Component	Concentration Range
Nitric Oxide (NO)	~ 200 – 800 ppm
Nitrogen Dioxide (NO_2)	~ 50 – 600 ppm
Nitrous Oxide (N_2O)	~ 20 – 300 ppm
Carbon Monoxide (CO)	~ 50 – 5000 ppm
Carbon Dioxide (CO_2)	~ 5000 ppm – 5%

The first step in analysis method setup is to determine analysis regions, the portions of the infrared spectrum that will use to quantify all the components in the method. First, measure a spectrum of each component at the highest concentration which are expect to be found in the samples. Then compare the spectra for all components and, for each component, choose at least one frequency range in which the component peaks are clearly identifiable. Do not choose a frequency range in which the component to be quantified is effectively opaque (absorbance units >1). Also avoid choosing a frequency range in which another component absorbs strongly. If interfering peaks occur in the selected frequency range for a component, select several small windows in which the component peaks are strong but less than 1.0 absorbance units and the interfering

component peaks are less than 0.5 absorbance. The region windows used to quantify the 5 gases used in experiments are showed in Table 2.3.

Table 2.3 Specified Regions of the Spectrum Where Each of the Components Absorbed

Region Window	Components				
	NO	NO_2	N_2O	CO	CO_2
1820.0 – 1920.0 cm^{-1}	S	-	-	-	-
2100.0 – 2158.0 cm^{-1}	-	-	-	S	I
2207.0 – 2220.5 cm^{-1}	-	-	S	I	I
2249.0 – 2255.0 cm^{-1}	-	-	I	-	S
2865.0 – 2931.2 cm^{-1}	-	S	-	-	-

- component does not absorb significantly in this region

I component absorbs significantly in this region

S use this region to calculate the concentration of this component

After finished defining the analysis region and calculation region for each component, it is time to calibrate the method. The initial method calibration is based on the assumption that all components have linear absorbance vs. concentration behavior (obey Beer's law). As a result, a single standard spectrum is used to develop a linear model that relates spectral features to method validation results show that the calculated concentration of a component differs from the actual concentration by more than an acceptable amount (usually 1 to 5 %), the absorbance vs. concentration plot for that component may be curved instead of linear.

The common calibration method involves preparation of surrogate samples or standards of known concentrations, covering the range of concentrations expected in experimental samples. The standards concentration should bracket the sample concentration, and should be as close to the samples as possible. The standards are analyzed on the instrument to be calibrated and the response is plotted against the known concentration. The plot is used to determine the amount of analyte in the unknown samples. If the response/concentration line is a straight line or is a curve with a readily determined equation, the equation of the line is often used to calculate the concentration in a sample, in place of the physically plotted data.

In this case, 3 different concentrations were used for each of the five components to cover their ranges. They are: 50, 500 and 1200 ppm of NO/He; 30, 100 and 250 ppm of N_2O/He; 50, 230 and 500 ppm of NO_2/He; 50, 250 and 450 ppm of CO/He; 5200 ppm, 2% and 5% CO_2/He. After collecting all spectrums, just save them and using the OMNIC QuantPad software to calculate the correlation curves for each of the component.

2.2.4 Chemical and Gases Used

Gases are Supplied by Matheson Gas Products. All gas mixtures were purchased as certified standards and included mass spectrographic verification of the mixture content.

NO: 50, 500, 1260 ppm in Helium

NO_2: 50, 250, 500, 1200 ppm in Helium

N_2O: 30, 101, 250 ppm in Helium

CO: 50, 250, 450, 1000 ppm in Helium

CO_2: 5200ppm, 2%, 5% in Helium

Oxygen: 99.995%

He: 99.995%

Catalyst: supplied by Engelhard Co.

Alumina: supplied by Engelhard Co.

Granular Activated Carbon: supplied by J.T.Chemical Company

$PdO(NO_3)_2.xH_2O$: supplied by Alfa Aesar (Pd 40.61%)

2.3 Experimental Procedure

This section of chapter 2 contains details of the experimental procedure.

2.3.1 Preparation of PdO/Al_2O_3 catalyst

Incipient wetness impregnation method described by Richardson, (1989) was used to synthesize metal loaded catalysts on the support materials mentioned before. This method fills the pores of the support particles with a solution of the desired metal salt of sufficient concentration to give the desired metal loading. In this research, gamma alumina was used as the support particles and $Pd(NO_3)_2$ was used as the metal salt. The support particles were pretreated by heating to remove all pore moisture and other adsorbed gases. The required volume of metal ion solution was determined by measuring the volume of deionized water that is adsorbed and confirmed by calculation of the volume from the measured pore volume, the maximum water which a certain mass of alumina can absorb is referred to as the water pore volume. To determine the water pore volume, deionized water was slowly added to a known mass of dried support materials until it was saturated as indicated by beading of excess water, i.e., no more water is adsorbed. The

measured volume of deionized water per unit mass of support material is used as the value of the water pore volume for the synthesis of catalyst by the incipient wetness impregnation method due to Richardson, (1989). The mass of cupric nitrate could be calculated by the known mass of support material and the percentage of Pd ion wanted. The support material was soaked in the exact volume of cupric nitrate solution, which was determined, by the water pore volume and the mass of the support materials over night. The slurry was then dried at 100°C for 5 hours to evaporate the water. The salt crystallized in the pores as the water was removed. Finally, the catalyst was calcined to convert the salt crystals in the pores to oxides. Crystallized salt redissolves when the dehydrated catalyst is exposed to moist environments. The purpose of the calcinations is to convert the salt to an oxide and "freezes" the distribution. The required calcination temperature was 500°C from relevant references and Xiao, et al. (1998). The temperature was determined by TGA experiment. A weight-percentage loss versus temperature was obtained that showed the temperature at which $PdO(NO_3)_2$ started to decompose to PdO. Gamma alumina supported catalysts were calcined in a furnace with air flowing for six hours at 500°C.

2.3.2 Catalyst Characterization

In heterogeneous catalytic reactions, a number of physical and chemical properties are very important for the catalysts to perform as required. In this thesis, BET surface area, Temperature Programmed Reduction (TPR) and CO chemisorption were measured using an Altamira AM-1 Instrument.

2.3.2.1 BET surface area: The BET surface area was measured using the Altamira Instrument, see figure 2.3. This nitrogen adsorption measurement was conducted by a continuous flow method (Nelsen, et al., 1958). This method does not require the use of vacuum as does the conventional static technique. Also, it can be extended to a lower range of surface areas, because of the high sensitivity of thermal conductivity detection. The experimental procedures for BET surface area measurements are as follows:

1. Load 0.5 g catalyst sample into quartz U-tube.

2. Install U-tube on the Altamira Catalyst Characterization Instrument.

3. Pre-treat the catalyst sample by using helium at 30 cm^3/min for 30 minutes.

4. Measure the vapor pressure of liquid nitrogen, P_o.

5. Measure the ambient pressure, P.

6. Introduce 10% N_2 in helium gas through the U-tube at 30 cm^3/min. once the TCD baseline is stable, immerse the sample tube onto the liquid nitrogen Dewar. Since the N_2 molecules condense onto the catalyst surface at liquid N_2 temperature, the response of TCD shows a negative peak. The TCD signal goes back to the baseline when nitrogen molecules saturated the catalyst surface. Remove the liquid nitrogen Dewar when the baseline is stable. The response of the TCD shows a positive peak when the temperature reaches room temperature. This peak indicates that the desorption of nitrogen molecules from catalyst is complete.

7. Inject two pulses of known volume of nitrogen into the carrier gas flow. Comparing the adsorption and desorption peak area with the calibration peak, one can obtain the actual volume of nitrogen adsorbed on the catalyst sample.

8. Repeat 6 and 7 with 20% N_2 in helium and 30% N_2 in helium adsorbate gas and measure the actual volume of N_2 adsorbed on the catalyst sample.

9. By rearrange following equation

$$P / V(P_o-P) = 1 / V_mC + (C-1)P / V_mCP_o$$

and plot $1 / V[P / P_o-1]$ versus P/P_o, a straight line was obtained $y = ax + b$, where a is the slope $(C-1) / V_mC$ and b is the intercept $1 / V_mC$.

V_m can be calculated as follows Altamira Instruction Manual 1989:

$$V_m = 1 / (\text{slope} + \text{intercept})$$

And the surface area is given by:

$$SA = V_mNA_{cs} / V'$$

Where:

SA = total surface area, m^2/g,

V_m = volume of adsorbate at monolayer coverage, cm^3/g,

N = Avagadro's number, $6.02* 10^{23}$ molecules / mol,

A_{cs} = cross section area of adsorbate molecule, 0.162 nm^2,

V' = molar volume of adsorbate at 25°C, 24500 cm^3/mol.

2.3.2.2 Temperature Programmed Reduction (TPR) and Chemisorption: Specific chemisorption methods have found considerable utility in determining the selective adsorption of a gas onto the active component of a supported catalyst. By using this method, one can understand the dispersion of active component on the carrier surface as well as metal surface area.

Pulse adsorption method is used in this research. An usual procedure is to unject a known volume of gas of known composition into a stream of carrier gas which pass through the catalyst bed. If the adsorbate is completely taken up by the catalyst, the detection system will not sense the change in thermal conductivity. When saturation of the catalyst is achieved, then additional adsorbate passes into the detector, and the area under the thermal conductivity response curve provides the volume of gas adsorbed. By knowing the composition of the adsorbate, pulse volume, and the number of pulses, one can calculate the volume of adsorbate per an unit weight of catalyst.

In the case of palladium adsorption, CO is preferred as the adsorbate in the pulse adsorption method (Farrauto, 1974). By assuming Pd-CO adsorption is linear, one can calculate the moles of Pd atoms on the surface of the catalyst. Dispersion is defined as (Heck and Farrauto, 1995):

$$\text{Dispersion} = \frac{\text{Number of catalytic sites on the surface}}{\text{Theoretical number of sites present}}$$

Basically, dispersion is an index which reflect crystalline size of active component on the surface of a substrate and is a diagnostic method used to understand how a catalyst is affected by some unusual condition such as high temperature, or presence of a poisons.

This experiment was conducted using the Altamira Instrument. A 0.5 g sample was packed in a U-tube for Temperature Programmed Reduction (TPR) and chemisorption. The flow schematic diagram for TPR is shown in Figure 2.2. The experimental procedure for TPR can be summarized as follows (Yu, 1991):

1. Load 0.5 g powder catalyst into U-tube.
2. Install U-tube on the Altamira Catalyst Characterization Instrument.

3. Set operating parameters:

Step 1: Temperature: 50°C

Carrier gas: Argon, 30 cm^3/min.

Step 2: Temperature: programmed temperature, 49 to 550°C, ramp rate 10°C/min,

Carrier gas: 5% H_2 in argon.

Step 3: Hold the temperature at 550°C for 30 minutes.

Step 4: Cool down to room temperature and shift carrier gas to argon.

Inject adsorbate gas, CO for 10 Pulses.

Step 5: Calculate total volume of CO adsorbed on the surface of the catalyst.

Step 6: Convert the volume of CO which adsorbed on the surface of catalyst per 0.5g to the volume of CO per gram.

2.3.3 Catalyst Testing

In these experiment, the contact between catalyst and soot is a very important factor for catalytic performance. It is known that one of the realistic systems for the catalytic reduction of PM is a PM trap loaded with catalyst. There are many technological difficulties in this system such as the development of an efficient and thermally stable PM trap, loading of catalytic materials on the trap and the contact between catalyst and the trapped PM.

For example, Neeft et al. (1997) investigated the influence of the type of the soot/catalyst contact in the soot oxidation reaction. They used three types of contact: "tight" contact by mechanical milling, " loose" contact by loose mixing with a spatula and " in-situ" contact by collecting soot on a catalyst placed in a diesel exhaust stream. In

their study, the combustion temperature of soot, which is defined as peak maximum temperature of differential scanning calorimetry (DSC) curve, is of comparable magnitude between the loose and in-situ systems, and the activity of the tight contact is far higher than that of the other two. These results demonstrate that the loose contact resembles the contact under practical conditions and that the improvement of the contact is crucial for the performance of the practical trap. So, all these experiments for catalyst activity testing and kinetics research were performed in the quartz fixed bed reactor with the loose mixture of catalyst and GAC placed on a porous quartz disk inside the reactor.

The whole system was heated to 150°C for about an hour under helium flow in order to remove impurities such as water which may have adsorbed on the solid materials. The gas cell for FTIR should also be purged thoroughly by pure helium flow for at least 2 hours until the background spectra shows no signs of water. Each gas flow was controlled by a needle valve based on the indicated flow rate from a calibrated set of rotameters. The desired operating temperature of the reactor was maintained by a temperature controller.

A small temperature jump of about 20°C was observed when switching all reactant gases from cylinders into the reactor at same time with the initial temperature below 450°C. When initial reactor temperature was 500°C, all GAC was consumed in a few minutes and the temperature went up to almost 700°C. In this case, we let the desired gaseous reactants, except O_2, flow through the whole experimental system for about 1 hour at first, in order to obtain a steady state temperature. Only then was the O_2 injected into the system just before collecting data. It also should be noted that as the GAC is consumed when NO and O_2 were introduced to the system, each experiment was

conducted with a fresh charge of catalyst and GAC in order to investigate the reactivity of GAC for NO reduction to nitrogen on an equivelent basis.

The GC used both a thermal conductivity detector (TCD) and a flame ionization detector (FID) to analyze the gaseous mixture. The TCD is used to measure the concentration of NO, NO_2, N_2 and O_2. The FID is used to determine CO and CO_2 concentration after separating these gases over a Porapak Q column and converting them to methane over a Ni catalyst. A different GC column is used with each detector. The column that is connected to the TCD is 0.32 cm in diameter by 9.14 m long stainless steel column packed with 100/120 mesh HayeSep DB. The column that FID connected is 0.32 cm in diameter by 2 m long stainless steel tube packed with 80/100 mesh Porapak Q. the results of the two analytical methods agree to within 10% and allow measurement of N_2 and O_2 which can not be measured by FTIR.

A Nicolet 520 FTIR equipped with a 2m gas cell was used for continuous analysis of NO, NO_2, N_2O, CO and CO_2. The instrument was calibrated with certified gaseous mixture in which He was the balance gas. In the catalyst testing, the feed and effluent gases from the system were measured by online FTIR at each 50°C in the range of 350 °C to 500 °C. 5 different space velocity experiments were conducted for activity test. The gaseous hourly space velocity (GHSV) was calculated by dividing the total gas flow rate (m^3/h) at the temperature and pressure of the experiment by the total solid sample volume (cm^3).

Space Velocity = Total flow rate / Solid sample volume

The higher the space velocity, the less the residence time of the reaction. The space velocity used in this research were 12,000, 24,000, 48,000 and 60,000. For the kinetics

research, the reaction gases with various partial pressure of oxygen and NO (P_{O_2}, P_{NO}) were obtained by adequately blending gas flow, the NO concentration used were 200, 300, 600 ppm, oxygen concentration were 3, 5 and 10%.

CHAPTER 3

RESULTS AND DISCUSSION

This section will provide the results from the experiments conducted to clarify the results of N_2 formation from the catalytic reaction of GAC with NO over PdO/Al_2O_3.

3.1 Catalyst Characterization

Specific BET surface area was measured by Altamira Instrument. The result of specific surface area and CO chemisorption for self-synthesized 2.5% loading PdO/Al_2O_3 catalyst shows in Table 3.1.

Table 3.1 Specific BET Surface Area and CO Chemisorption for 2.5% $PdO/\gamma\text{-}Al_2O_3$ Catalyst

	Specific BET Surface Area (m^2/g)	CO chemisorption (cm^3/g)	Percent Dispersion
Plain $\gamma\text{-}Al_2O_3$	216	0	0
$PdO/\gamma\text{-}Al_2O_3$	175	11.3	21

3.2 Reduction of NO by Granular Activated Carbon (GAC) over $PdO/\gamma\text{-}Al_2O_3$

The catalytic activity needed to promote the reduction of NO by GAC to nitrogen gas was measured in a down-flow reactor system illustrated in figure 2.1. The feed gas, which contained the essential reactive components in order to simulated diesel exhaust gas, was composed of 600 ppm NO, 5% oxygen and helium as the balance gas. The reactor bed was composed of catalyst and GAC at a volume ratio 1:1. Activity test were conducted at a gaseous hourly space velocity (GHSV) of 24,000 and the effluent gas was analyzed by FTIR for NO, NO_2, N_2O, CO and CO_2 and by GC for N_2 and O_2, using fresh

mixtures of GAC and catalyst. Runs were conducted at the following temperatures: 350, 400, 450 and 500°C. The conversion of NO to nitrogen is determined by difference between nitrogen atoms fed to the catalytic reactor, NO inlet minus all effluent nitrogen atoms ($NO + NO_2 + N_2O$) outlet divided by the inlet nitrogen atoms and calculated according to equation 1.

$$\text{Conversion (\%)} = \{NO_{\text{inlet}} - (NO + NO_2 + N_2O)_{\text{outlet}}\} / NO_{\text{inlet}} \quad (1)$$

As indicated in Chapter 2, experimental, the inlet gas mixture contained no nitrogen gas. The essentially inert nitrogen was replaced with He in order to independently check the quantity of nitrogen formed from NO using GC with TCD. The results presented in Table 3.2 show that the two methods of measuring N_2 are consistent, i.e., by difference (FTIR) and direct (GC).

Table 3.2 Summary of the Results Obtained for a GHSV of 24,000 as a Function of Temperature

Peak Temp. (°C)	Initial Temp. (°C)	Inlet NO (ppm)	Outlet NO (ppm)	Outlet NO_2 (ppm)	Outlet N_2O (ppm)	Conversion (%) by FTIR	Conversion (%) by GC
350	350	625.	480	37.2	7.32	7.72	3.20
410	400	622	457	34.5	18.7	12.4	7.34
467	450	619	363	28.6	24.9	25.0	17.8
639	500	625	183	0	37.6	70	78.9

In heterogeneous catalytic reactions, the overall reaction process can be separated into a sequence of individual steps which are shown below (Heck and Farrauto, 1995):

1. Mass transfer of the reactants from the bulk fluid to the external surface of the catalyst.

2. Diffusion of the reactant from the pore mouth through the catalyst pores to the immediate vicinity of the internal catalyst surface.

3. Adsorption of reactant onto the catalyst surface.

4. Reaction on the surface of catalyst.

5. Desorption of the products from the surface.

6. Diffusion of the products from the interior of the catalyst to the pore mouth at the external surface.

7. Mass transfer of the products from the external catalyst surface to the bulk fluid.

The overall reaction rate is determined by the slowest step in the mechanism. In the chemical kinetic region, where the diffusion steps 1, 2, 6, 7 are fast compared to the reaction step, the reaction rate is proportional to the negative exponential of inverse temperature, the proportionality constant is referred to as the activation energy. So, the rate of conversion increases with temperature. In pore diffusion region, steps 1, 3, 4, 5, 7 are fast compared to diffusion step 2 and 6, the rate is proportional to the square root of the negative exponential of inverse temperature. Hence, the rate of conversion increases with temperature but is less sensitive to temperature compared to the chemical kinetic control region. In bulk mass transfer region, step 2, 3, 4, 5, 6 are faster than the bulk mass transfer step 1 and 7. The rate equation in the mass transfer control region is almost linear, i.e., independent of temperature (Fogler, 1986). And the corresponding activation energies should have values on the order of:

Chemical kinetics, Ea > 10 kcal/mol

Pore diffusion, Ea = 6-10 kcal/mol

Bulk mass transfer, Ea = 2-4 kcal/mol

As show in table 3.2, the PdO/Al_2O_3 catalyst exhibited low activity below 400 °C. The conversion rate of NO to N_2 increased with increasing temperature, it appears that the catalytic reactions are controlled by chemical kinetics in this region. After that, there was a sudden change in conversion rate from 20% of 450°C to 70% of 500°C, which appears to be in the diffusion controlled regions. After that the conversion rate did not increase significantly with increasing temperature indicating that the reaction was controlled by mass transfer.

The data in Figures 3.2 to 3.5 clearly show that results in the temperature range of 350 to 450°C, the reaction reach as a steady state very soon after injecting oxygen into the feed gas stream. The concentration of NO and NO_2 in the effluent gas decreases as the temperature is increased. A very small amount of N_2O, about 20 ppm, was detected in the outlet stream indicating that the reduction of NO to nitrogen by GAC with oxygen present is not the only reaction. When the catalyst temperature is increased to 500°C, the reaction becomes very fast after injection of oxygen and the reaction temperature increase sharply to almost 700°C because the GAC-oxygen reaction is very exothermic. The reaction returns to the initial catalyst temperature in several minutes when all the carbon is consumed. It is therefore necessary to reload fresh mixture of GAC and catalyst after each kinetic measurement. From figure 3.5, it can be seen at the point of oxygen injection, the NO concentration suddenly decrease to 185 ppm and CO_2 increase sharply at same time. The oxides of nitrogen concentration in the effluent gas, namely ($[NO]+[NO_2]+2[N_2O]$), become very small when compared with the inlet concentration of NO. Integrating the decrease of the concentration of CO_2 to zero after 3 hours, one obtains the total GAC that is oxidized. Here again there is a good agreement between

GAC loaded in the flow reaction and the CO_2 produced. It should be noted that there is another smooth peak of N_2O showed in outlet effluent in about 10 minutes after injection of oxygen. This is supposedly due to the fact that the catalytic reactions involving carbon take place at the three-phase boundary of a solid catalyst, solid soot and gaseous reactants.

It is assume that the adsorbed species on the catalyst surface are formed at the boundary or spill over from the remote sites to the boundary, and a part of carbon in close vicinity takes parts in the reaction. Gaseous oxygen is adsorbed dissociatively on the catalyst surface and resulting in atomic O_{ad} adsorption that react rapidly with the reactive free carbon site to give an oxygen-containing active intermediate, C*[O]. Suzuki et al. (1993) examined the carbon surface after the reaction with a gaseous mixture of NO and oxygen by X-ray photoelectron spectroscopy and confirmed the pressure of the following nitrogen groups complexed with carbon: pyridinic, pyrrolic, -NO, $-NO_2$. The former two and latter two groups might correspond, respectively, to C*[N] and C*[N, O] intermediates involved in the reaction. So, the late N_2O peak may suggest that there were a lot of [NO*] and C*[O] species adsorbed on the porous solid material before they reacted according to following equation:

$$C^*[O] + 2[NO^*] = N_2O + CO_2 \qquad (2)$$

It also implies that the formation of nitrogen and N_2O are competitive reactions with the common intermediate of NO_{ad}. The competing reactions are:

$$C^*[O] + [NO^*] = [N^*] + CO_2 \qquad (3)$$

$$[N^*] + [N^*] = N_2 \qquad (4)$$

3.3 Effect of Space Velocity

The effect of space velocity was investigated by changing the total gas flow rate while keeping the volume of the catalyst powder used constant. The solid materials is placed in the reactor contain well mixed PdO/Al_2O_3 and GAC at a volume ratio of 1:1. The total catalyst volume is 2 cm^3. The calculation of GAC, flow rate of NO, O_2 and residence time is listed below:

Weight of 1 cm^3 2.5% PdO/γ-Al_2O_3: 0.3598 g

Weight of 1 cm^3 GAC: 0.4054 g

NO concentration: 600 ppm

When GHSV = 12,000/hr total flow rate: 200 cm^3/min

Flow rate of 1220 ppm NO: 100 cm^3

Flow rate of 10% O_2: 20 cm^3/min

Residence time = 1/[(12,000/hr)*(1hr/3600 s)] = 0.3 s

Figures 3.6 and 3.7 compare the effect of gaseous hourly space velocity (GHSV) for the NO/O_2/GAC system. The five curves represent the conversion of NO to N_2 with temperature in the range of 350°C to 500°C at 12,000, 24,000, 48,000, 60,000 and 90,000 GHSV. The results show that space velocity which is the inverse of resident time, has an important effect on the reduction of NO. Residence time for the GHSV studied are summarized in Table 3.3.

Figure 3.7 shows that light off temperature is on the order of 300°C and does not change with GHSV from 12,000 to 90,000. Although conversion to nitrogen as a function of temperature decreases as the GHSV increases, the conversion is still 70% at a GHSV of 90,000. For the reaction at 12,000 GHSV, the reaction rate is very sensitive to

temperature in the range of 300°C to 400°C, where 6 and 22% NO conversion to N_2 is obtained at 350°C and 400°C respectively. However, at 450°C and 500°C, the conversion of NO to nitrogen increases to 50% and 90%, respectively. The 12,000 GHSV curve in figure 3.6 goes through the expected rate controlling transitions from kinetic control (300 to 350°C) through diffusion control (350 to 500°C) and levels out above 500°C in the mass limited region at 90% conversion to N_2.

Table 3.3 Calculation of Residence Time for Five Different GHSV Used in This Study.

GHSV	Residence time (second)	Total flow rate (cm^3/min)	NO flow rate (cm^3/min)	O_2 flow rate (cm^3/min)
12,000	0.3	200	100	20
24,000	0.15	400	200	40
48,000	0.075	800	400	80
60,000	0.06	1000	500	100
90,000	0.04	1500	750	150

To a first approximation, the three rate controlling mechanisms occur over the same temperature ranges for all 5 GHSV presented in figure 3.6. Detailed research needs to be conducted over the temperature range over which the rate controlling transitions occur. This will allow better estimates of the maximum conversion. It can be seen in Figure 3.7 that there are insufficient points to adequately establish the chemical kinetics regime because of the difficulty in running at very high GHSV, i.e., short space time in the reactor. Most of the measurements explain the diffusional-controlled region.

Suzuki et al. (1993) reported that the coexistence of NO and oxygen can enhance the oxidation of soot with the intermediate C*[O]. This intermediate can react with either O_{ad} or NO_{ad} to produce CO_2 and nitrogen and plays an important role in the reduction. An

alternate mechanism is proposed by Xiao et al. (2001), which is based on the formation of strongly adsorbed CO. However, the curves of the component in the gas phase recorded with the on-line FTIR, no trace of CO was found at low space velocities. Only at sufficiently high temperature of 500°C and high GHSV of 60,000, does a sharp CO peak appear at the same time as the CO_2 peak. This observation is summarized in Figure 3.8. Also, no N_2O peak is seen in the effluent stream after oxygen is injected. The N_2O concentration is almost zero during the whole reaction. Similar results are observed at 90,000 GHSV. These results are consistent with the Xiao et al. (2001) mechanism.

3.4 Calculation of activation energy

The ability of a catalyst to increase a reaction rate can be measured by obtaining the Arrhenuis parameters. The activation energy of the reaction is the key figure of merit for comparing reaction rates. The catalyzed reaction usually involves three rate processes: (1) adsorption, (2) the formation and breakup of an activated complex, and (3) desorption of products. Each of these has its own activation energy. The rate of reaction is also determined by the number of active site and by the concentration on the catalyst surface of various adsorbed species. From the calculation of apparent activation energy of a reaction, it may be easier gain insight on a possible mechanism and identify the rate-controlling step.

The formation rate of each product can be written by the conventional Arrhenius-type power-law expression as follows:

$$r = A \exp(- Ea / RT)\, Cc^{n_1} C_{NO}^{n_2} C_{O2}^{n_3} \qquad (5)$$

$$\text{or} \quad \ln r = - Ea / RT + \ln A + n_1 \ln Cc + n_2 \ln C_{NO} + n_3 \ln C_{O2} \qquad (6)$$

According to the Arrhenius equation, the rate constant can be described as first order as follows:

$$k = A \exp(-Ea/RT) \quad (7)$$

where:

A is the pre-exponential factor, cm^3/g cat.-s,

Ea is the apparent activation energy, kcal/mol,

R is gas constant, kcal/mol-K

Ci is the concentration, mol/cm^3

n_i is the reaction order of each reactant and product that participate in the rate limiting step

k is rate constant, mol/g cat.-s,

Although the reaction orders have not been reported, it is generally assumed that the reaction order in soot concentration should be zero in the temperature range of this study. The linear relation between ln r and T^{-1} suggests that Equation (6) can be simplified to Equation (8) and that $\ln A\sum C_i$ and Ea can be obtained from the slope and the intercept for each reactant.

$$\ln r = - Ea / RT + \ln A\sum C_i \quad (i = C, NO, O_2) \quad (8)$$

Figure 3.7 shows plot of conversion versus W/V (where W is the mass of catalyst and V is the gas flow rate) for the NOx reduction with GAC over PdO/Al_2O_3 catalyst on the temperature range of 350°C to 450°C (typical conversions were below 30% thus minimizing product reactant reactions). Reaction flow rate were varied to change space time. By using linear regression method, one can solve for rate constant k. Ea and A are

obtained from the slope and intercept from a plot of the logarithm of the rate constants versus 1/T for the reaction (Figure 3.13).

$$\ln k_1/k_2 = - E/R\ (1/T_1 - 1/T_2) \qquad (9)$$

Figure 3.7 shows that at lower temperature of 350°, 400°C and 450°C, it is reasonable use the result points to make linear regression to calculate rate constants k at each temperature. But for 500°C, as mentioned above, the reaction occurs very rapidly and carbon is consumed within a minute. Thus, the conversion exceeds 30% by a wide margin. Also, due to the limitation of the reaction apparatus, we could not reach shorter space time for more accurate linear regression at 500°C. We arbitrarily assumed that the first point at about 70% conversion is representative of the kinetic regime. This is borne out by finding the point in reasonable agreement with the other points at lower temperatures. The Ea is calculated by Equation 9 in the temperature range of 350° to 500°C and the result is 24.1 kcal/mol (99.2 kJ/mol), which indicates that in the temperature range of 350 to 500°C, the reaction is kinetically controlled (Figure 3.13).

3.6 Mechanism of soot-NO-oxygen Reaction

Kagawa et al. (1997) investigated the catalytic combustion of soot deposits from diesel-powered engines and proposed following mechanism of soot-O_2 reaction to account for the observed half-order kinetics with respect to the oxygen partial pressure.

$$O_2\ (g) \leftrightarrow 2O_{ad}$$

$$C_f + O_{ad} \rightarrow C^*[O]$$

$$C^*[O] + O_{ad} \rightarrow CO_2\ (g)\ (+ C_f)$$

The detail of the C*[O] intermediate is unclear, but the presence of such an oxygen-containing reactive surface complex was confirmed on the char surface after reaction with gaseous oxygen.

As described in Appendix A, the rates of nitrogen formation are proportional to $P_{NO}^{1.75\text{-}2.77}$ $P_{O2}^{0.31\text{-}0.40}$ in the temperature range of 350 to 450°C, which corresponds to diffusion control. It indicates that the oxidation of soot was enhanced by the coexistence of NO and oxygen. One possible explanation of this phenomenon is the participation of NO_2. NO_2 is formed through the reaction of NO and O_2 possible in gas phase and then adsorbed dissociatively on the catalyst surface to form adsorbed NO_{ad} and O_{ad} species. The reaction between adsorbed O_{ad} and reactive C_f species give the C*[O] intermediate which is reactive toward the reduction of adsorbed or gaseous NO species.

$$NO(g) + \tfrac{1}{2}\, O_2 \rightarrow NO_2(g)$$

$$NO_2(g) \rightarrow NO_{ad} + O_{ad}$$

$$C_f + O_{ad} \rightarrow C^*[O]$$

The complicated dependence of the formation rates on partial pressures implies that the mechanism of the simultaneous NOx-soot removal is not straightforward. It should be noted here that the above mechanism of the reaction is tentative. That is, the participation of gaseous NO in step of CO_2 formation and nitrogen formation cannot be excluded. The CO_2 formation step with the participation of gaseous NO can be written as follows:

$$C^*[N, O] + NO\ (g) + 2\ C_f \rightarrow CO_2 + 2\ C^*[N]$$

Also probable is the participation of gaseous NO in the nitrogen formation step like:

$$C^*[N] + NO\ (g) \rightarrow N_2\ (g) + C^*[O]$$

Figure 3.14 Reaction scheme of the simultaneous soot-NO removal in $NO+O_2$ gas

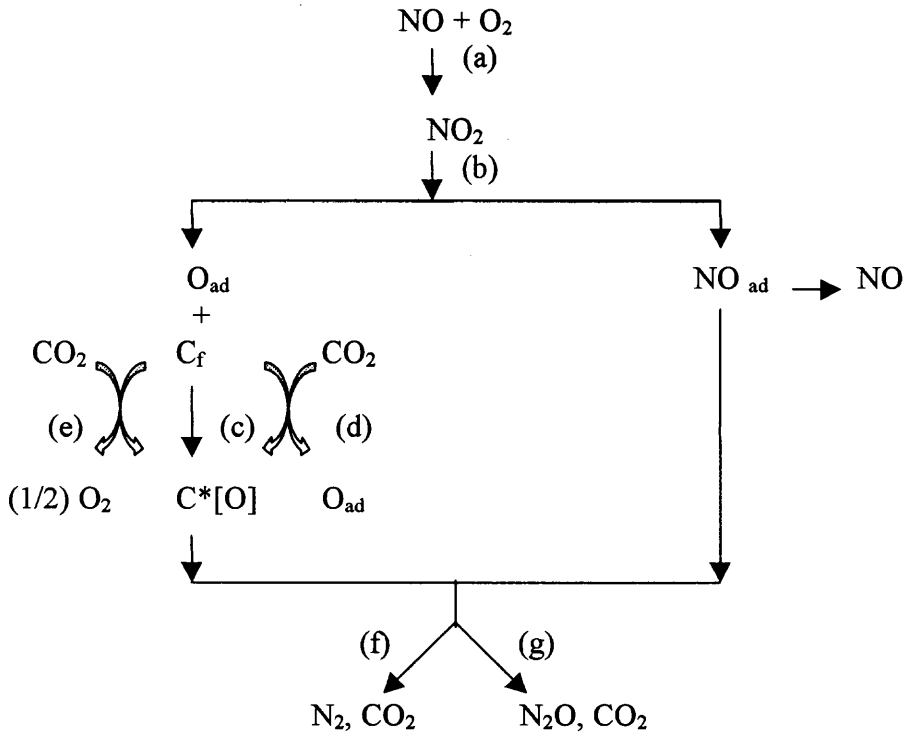

Based on these assumptions and the kinetics results, the reaction mechanism of the soot-NO-O_2 (simultaneous NOx – soot removal) reaction is proposed. In this mechanism, coexisting oxygen plays two crucial roles. One is the oxidation of NO probably in the gas phase to give NO_2 (step (a)) which has stronger oxidizing ability and easily gives adsorbed oxygen (step (b)), and the other is to propagate the C_f species by directly attacking the C*[O] intermediate from the gas phase (step (e)). Since major part of soot is consumed by the oxidation with oxygen in the soot-NO-O_2 reaction as stated before, the step (e) proceeds fast and contributes to increase population of not only the C_f species but also the active C*[O] species. The increasing population of C*[O] should result in the enhancement of the reaction between C*[O] and NO_{ad} to finally give nitrogen (step (f)) and N_2O (step (g)). In the scheme, the steps (f) and (g) are oversimplified. As can be

speculated from the results of soot-NO reaction, these reactions surely proceed by way of some intermediates such as C*[N, O] and C*[N].

CHAPTER 4

CONCLUSIONS

The catalytic reduction of nitric oxide by granular activated carbon in the presence of oxygen can be seen as three portion: chemical kinetic control in lower temperature, after 450°C, the reaction process is controlled by diffusion and mass transfer.

The reactions were taken place at the three-phase boundary of a solid catalyst, PdO/Al_2O_3, solid soot, GAC, and gaseous reactants. Hence, the adsorbed species on the catalyst surface play an important role in this reaction and are the focus for the future research.

The conversion of NO to nitrogen decreases as the GHSV increases. The highest conversion is 90% at space velocity of 12,000. The result are in excellent agreement with results presented in the references, which shows that PdO/Al_2O_3 is a good candidate for future research. Coexistence of NO and oxygen can enhance the oxidation of granular activated carbon and the intermediate C*[O] is formed in the three-phase reaction system. This result is in agreement with the results presented here.

From the reduction of NO with GAC over PdO/Al_2O_3 catalyst conversion curve and the ln(rate) vs. $\ln(P(NO)/P(O_2)$, the apparent reaction order is calculated as follows:

Rate $(N_2) \propto P(NO)^a P(O_2)^b$ which a=1.75 – 2.77, b=0.34 (GHSV=24,000)

Temperature range: 350 – 450 °C

The activation energy is calculated from the arrhenius plot. It was found that the activation energy for the reaction was 24.1 kcal/mol.

From above conclusion , the mechanism of reaction is:

$NO + O_2 = NO_2$

$O_2 (g) \leftrightarrow 2O_{ad}$

$C_f + O_{ad} \rightarrow C^*[O]$

$C^*[O] + O_{ad} \rightarrow CO_2 (g) (+ C_f)$

$NO_2 (g) \rightarrow NO_{ad} + O_{ad}$

$NO_{ad} + C_f \rightarrow C^*[N] + C^*[O]$

$C^*[O] + NO_{ad} + 2\ C_f \rightarrow CO_2 (g) + 2\ C^*[N]$

$C^*[O] + NO (g) + 2\ C_f \rightarrow CO_2 + 2\ C^*[N]$

$C^*[N] + NO (g) \rightarrow N_2O (g) + C^*[O]$

$2\ C^*[N] \rightarrow N_2 (g) + 2\ C_f$

It is recommended that the future research should be focused on the surface examination as the intermediate, C[O], formed on the solid surface. The intermediate plays an very important role in the whole reaction, which can be derived from the kinetics result, but stronger evidences should be obtained from more advanced surface research, such as in-situ FTIR, TPD/TPR. This may also help distinguish between CO as an intermediate, vs., adsorbed oxygen on GAC as the intermediate.

APPENDIX A

Rate Law Dependence on NO and Oxygen Partial Pressure in the Diffusion Control Zone

Takasa and Kagawa et al. (1998) reported that the effect of the amount of soot loading on C-NO-O_2 reaction over Cu-ZSM-5 and $CuFe_2O_4$ catalysts was insignificant. It appears that the C-NO-O_2 reaction is zero order with regard to the carbon loading in the presence of excess oxygen. Reaction mechanism will be discussed on the basis of the observed dependence on partial pressures of the rates of soot-NO-O_2 reaction in this appendix. This observation is consistent with the theory that gas-solid reactions are zero order in the solid because the reactions are dependent on surface and not concentration.

Due to the difficulty of reaching short spacetime as mentioned in Section 3.4, it is difficult to calculate the reaction orders in the kinetic control zone. To get insight on the reaction mechanism, experiments were conducted at 24,000 GHSV, which was believed in the pore diffusion control zone. The effect of concentration of the two gaseous reactants on the rate of simultaneous removal NO-soot was studied over PdO/Al_2O_3 at 350, 400 and 450°C. Two sets of experiments were carried out by varying NO concentration from 350 to 600 ppm and oxygen concentration from 3% to 10%.

The activation energy under this GHSV is 8.97 kcal/mol, which implies that these results are in the pore diffusion control zone.

The rate was calculated according to the following equation:

$$r_{nitrogen} = C_{NO} * Q * X / M$$

where: C_{NO} = inlet NO concentration (ppm)

Q = total flow rate (cm^3/min)

X = conversion (%)

M = mass of the catalyst (g)

The rates, r, of NO + O_2+ soot are listed in Tables 1 to 3. The reduction of NO with GAC over PdO/Al_2O_3 catalyst conversion curve and ln(rate) vs. $\ln[C_{NO}/C_{O_2}]$are showed in figure 3.9-3.12. The reaction order can be calculated from following equation:

$$r = k\, C_{NO}^{m}\, C_{O_2}^{n}$$

where: m is apparent reaction order of NO

n is apparent reaction order of O_2

Table 1 Influence of the partial pressure of reactants on the activity of PdO/Al_2O_3 on the soot-NO-O_2 reaction at 350°C, GHSV=24,000

C_{NO} (ppm)	C_{O_2} (%)	Conversion (%)	ln (Rate, mol g^{-1} h^{-1})
200	10	2.3	-2.85
300	10	5.2	-2.03
600	10	7.2	0.15
600	5	6.4	0.01
600	3	5.2	-0.23

Table 2 Influence of the partial pressure of reactants on the activity of PdO/Al_2O_3 on the soot-NO-O_2 reaction at 400°C, GHSV=24,000

C_{NO} (ppm)	C_{O_2} (%)	Conversion (%)	ln (Rate, mol g^{-1} h^{-1})
200	10	7.14	-1.65
300	10	11.1	-0.815
600	10	16.3	0.57
600	5	14.14	0.26
600	3	10.7	0.05

Table 3 Influence of the partial pressure of reactants on the activity of PdO/Al_2O_3 on the soot-NO-O_2 reaction at 450°C, GHSV=24,000

C_{NO} (ppm)	C_{O_2} (%)	Conversion (%)	ln (Rate, mol g^{-1} h^{-1})
200	10	19.56	-0.73
300	10	28.24	0.046
600	10	32.34	1.2
600	5	27.48	0.9
600	3	22.12	0.81

Table 4 Influence of the partial pressure of reactants on the activity of PdO/Al_2O_3 on the soot-NO-O_2 reaction at 500°C, GHSV=24,000

C_{NO} (ppm)	C_{O_2} (%)	Conversion (%)	ln (Rate, mol g^{-1} h^{-1})
200	10	19.56	-0.73
300	10	28.24	0.046
600	10	32.34	1.2
600	5	27.48	0.9
600	3	22.12	0.81

In each case, positive values for NO and oxygen orders are obtained. The apparent reaction order is obtained from these data by linear regression analysis with respect to the power law expression of the type are reported in Table 5. Under the experimental conditions, the positive NO and oxygen reaction orders indicates that the oxygen and NO enhance the reaction rate. The average of O_2 order is 0.34, which is similar to Teraoka et al (1998) result. The NO order is decreased from 2.77 to 1.75 as temperature increased from 350 to 450°C, which indicate that high temperature is advantageous for pore diffusion for the reaction.

Table 5 Apparent orders for the GAC-NO-O_2 reactions for PdO/Al_2O_3 catalyst at GHSV= 24,000

Reaction	Reaction order	Remarks
Soot-NO-O_2	$R(N_2) \propto P(NO)^{2.77} \quad P(O_2)^{0.30}$	T=350°C
	$P(NO)^{2.01} \quad P(O_2)^{0.41}$	T=400°C
	$P(NO)^{1.75} \quad P(O_2)^{0.31}$	T=450°C

It is difficult to compare these experiments orders with those reported in the literature by several investigators, since the dependence of the rate on the NO and oxygen concentrations is influenced by the nature of the catalyst and by the experimental conditions (temperature, reactant concentration ranges).

APPENDIX B
Figures

Figure **Page**

Figure **Page**

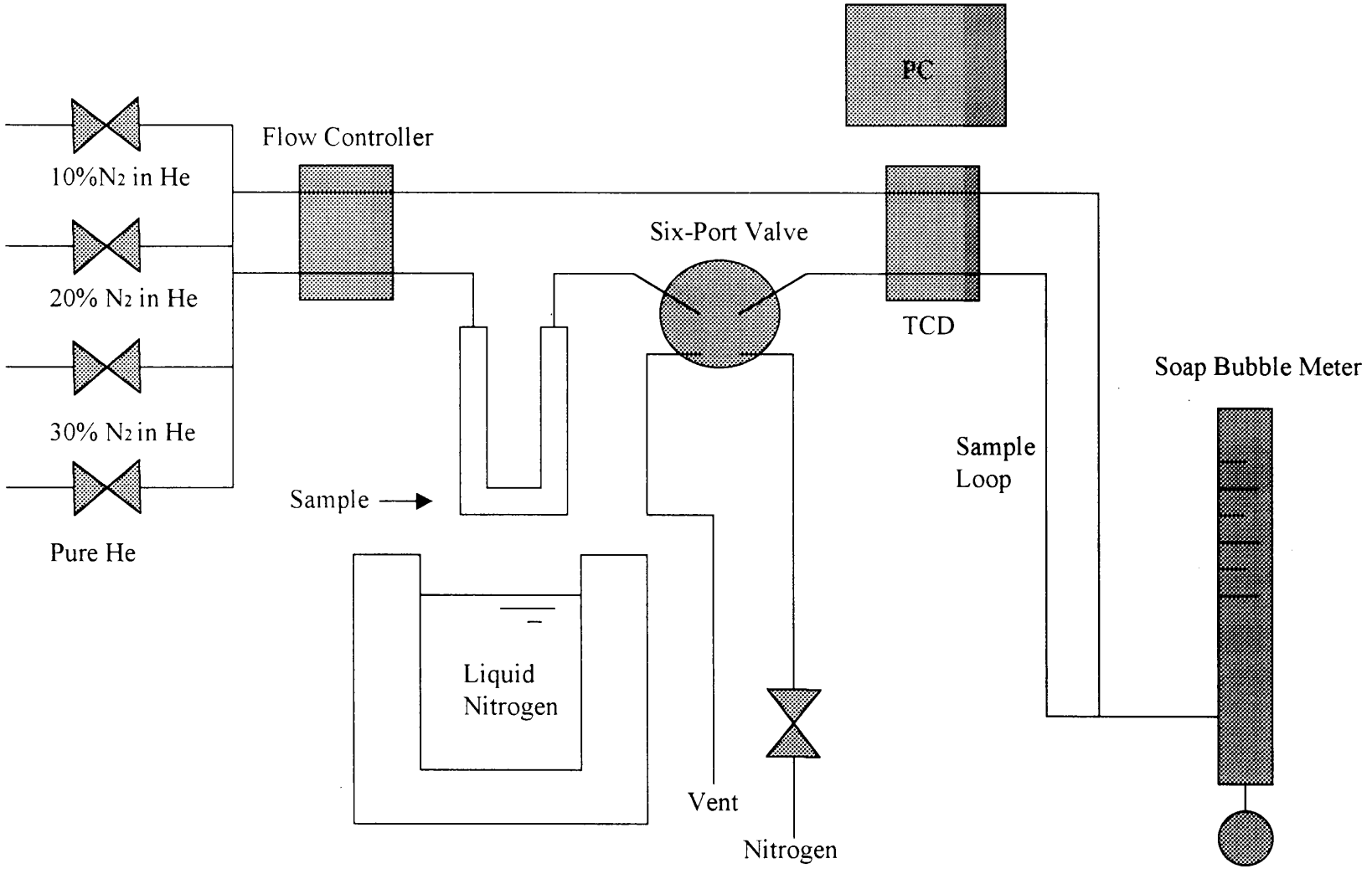

Figure 2.2 Flow Schematic Diagram of Altamira Instruments for BET Surface Area Measurements.

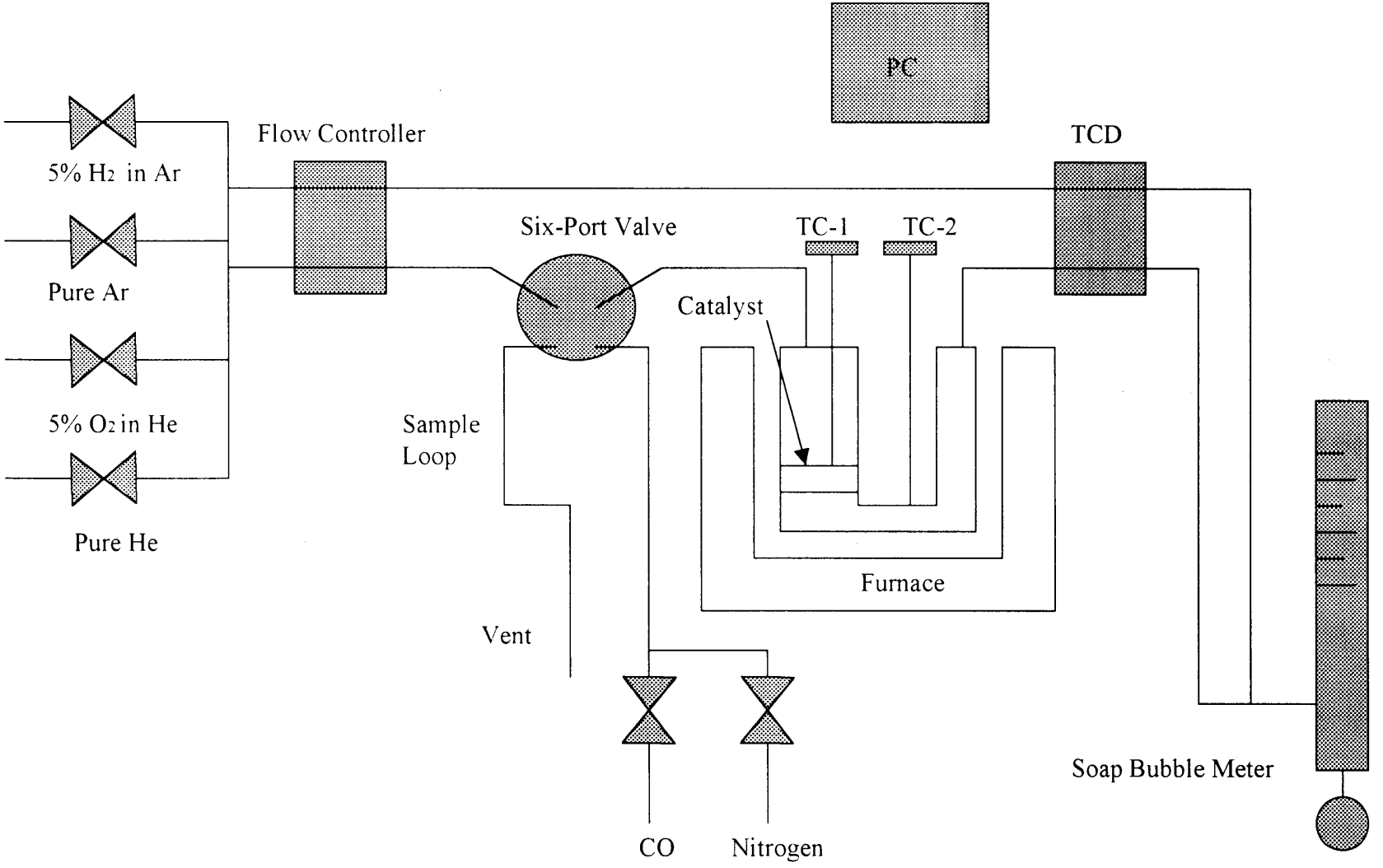

Figure 2.3 Flow Schematic Diagram of Altamira Instruments for TPR

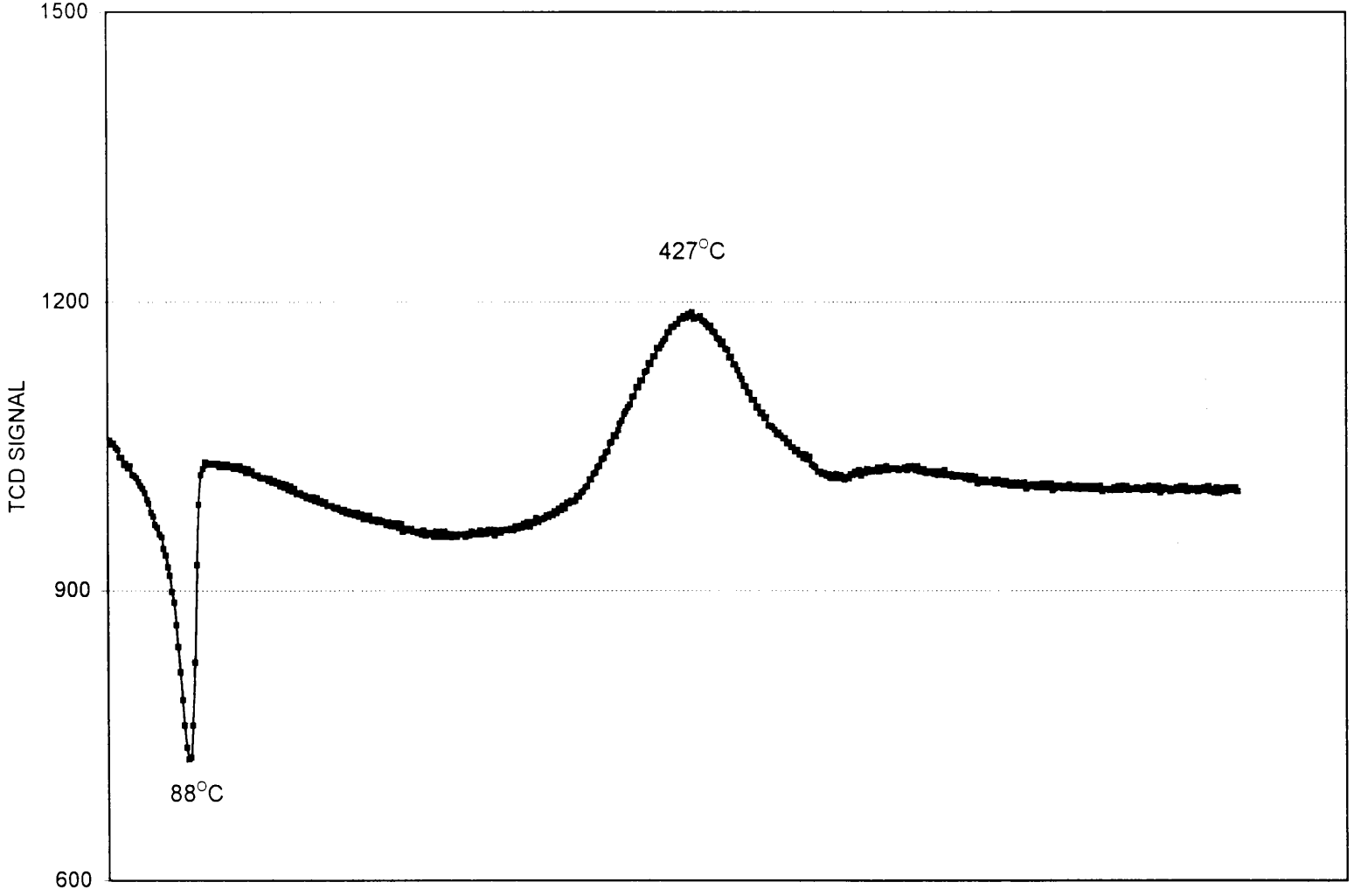

Figure 3.1 TPR of 2.5% Loading PdO/Al_2O_3 Catalyst by Altamira Instrument

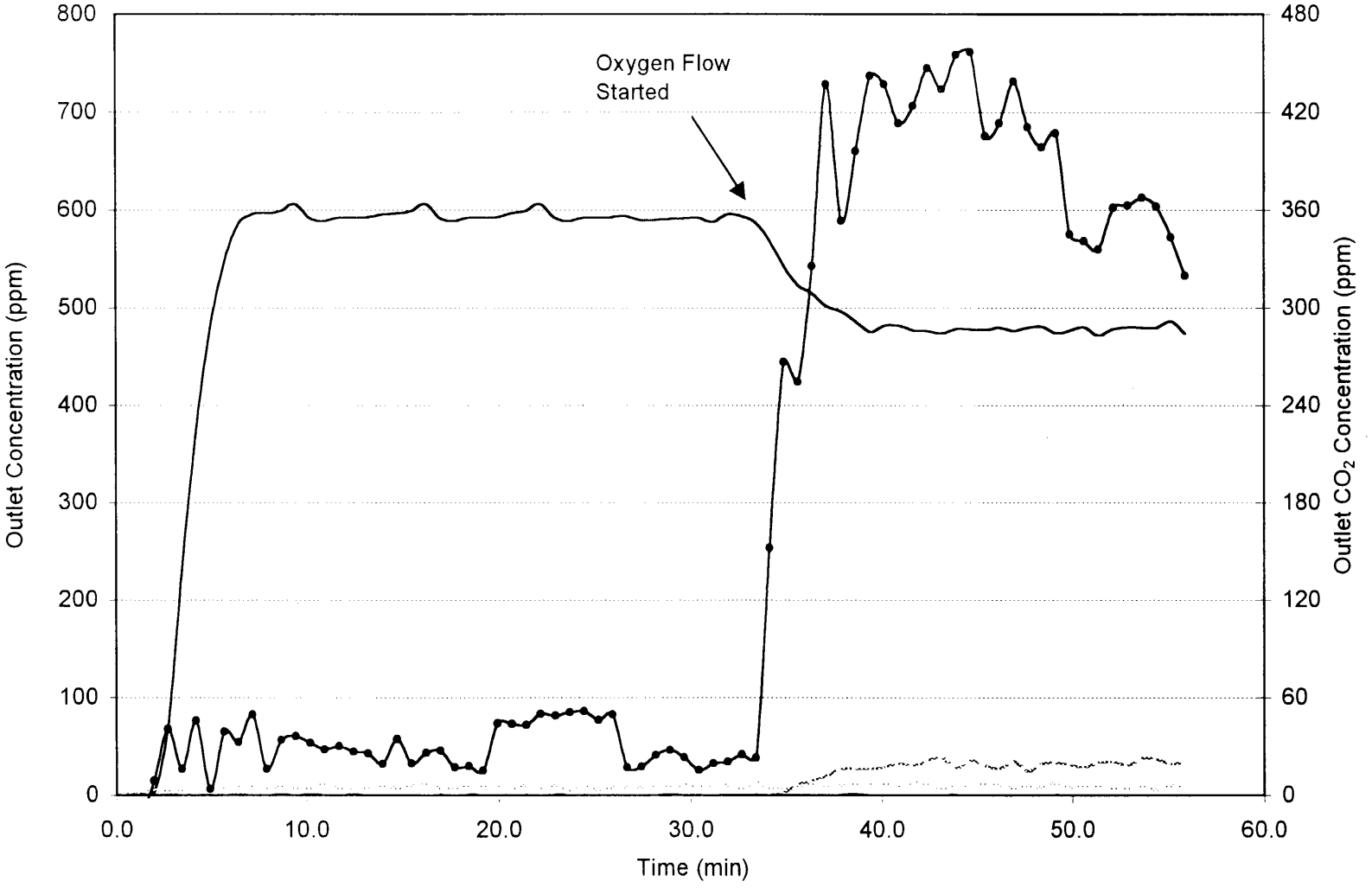

Figure3.2 Reduction of NO with GAC over PdO/Al_2O_3 Catalyst, GHSV= 24,000 [NO]=596 ppm, O_2=5%, GAC, Initial Temperature= 350°C

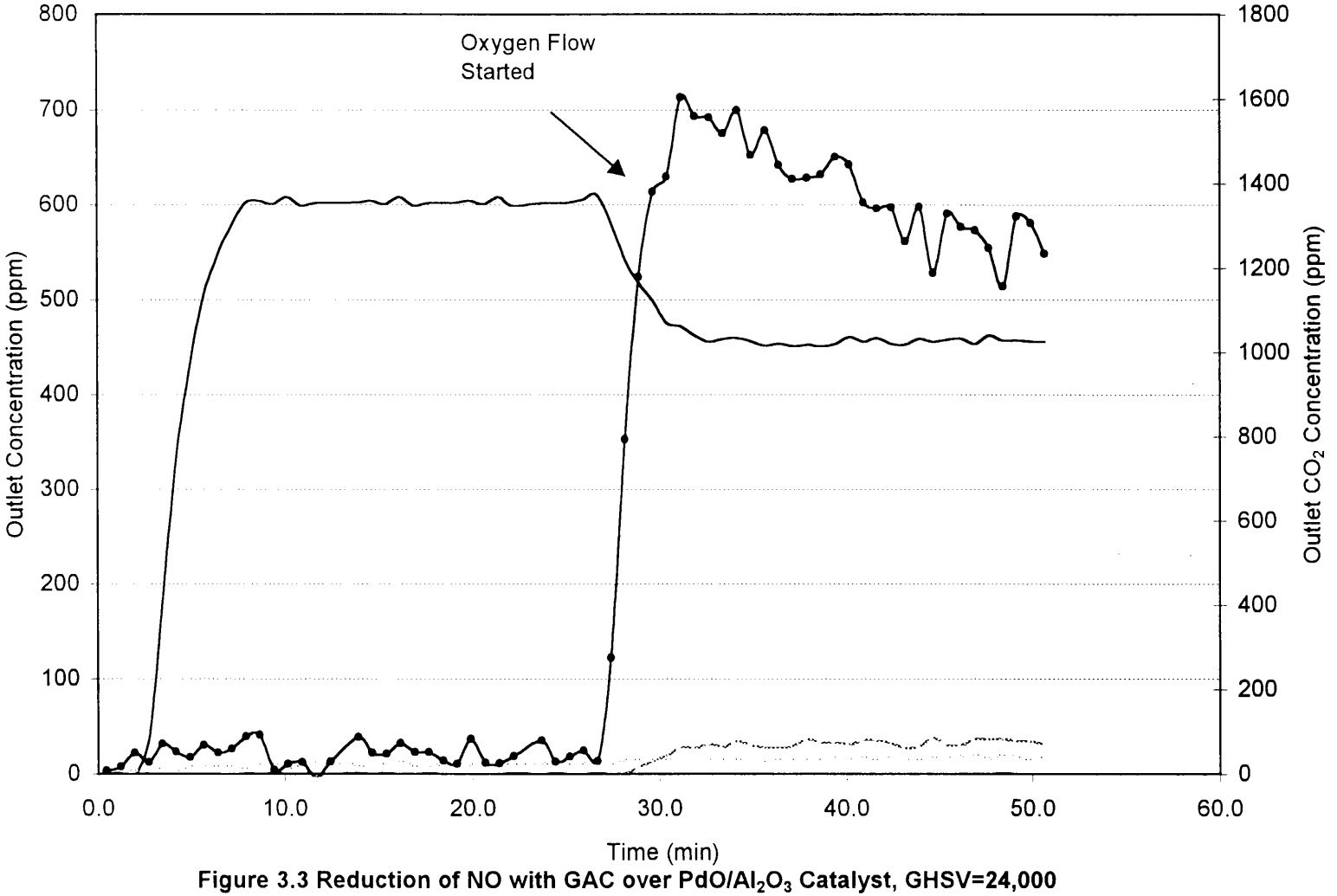

Figure 3.3 Reduction of NO with GAC over PdO/Al_2O_3 Catalyst, GHSV=24,000 [NO]=596ppm, O_2=5%, Initial Temperature=400°C

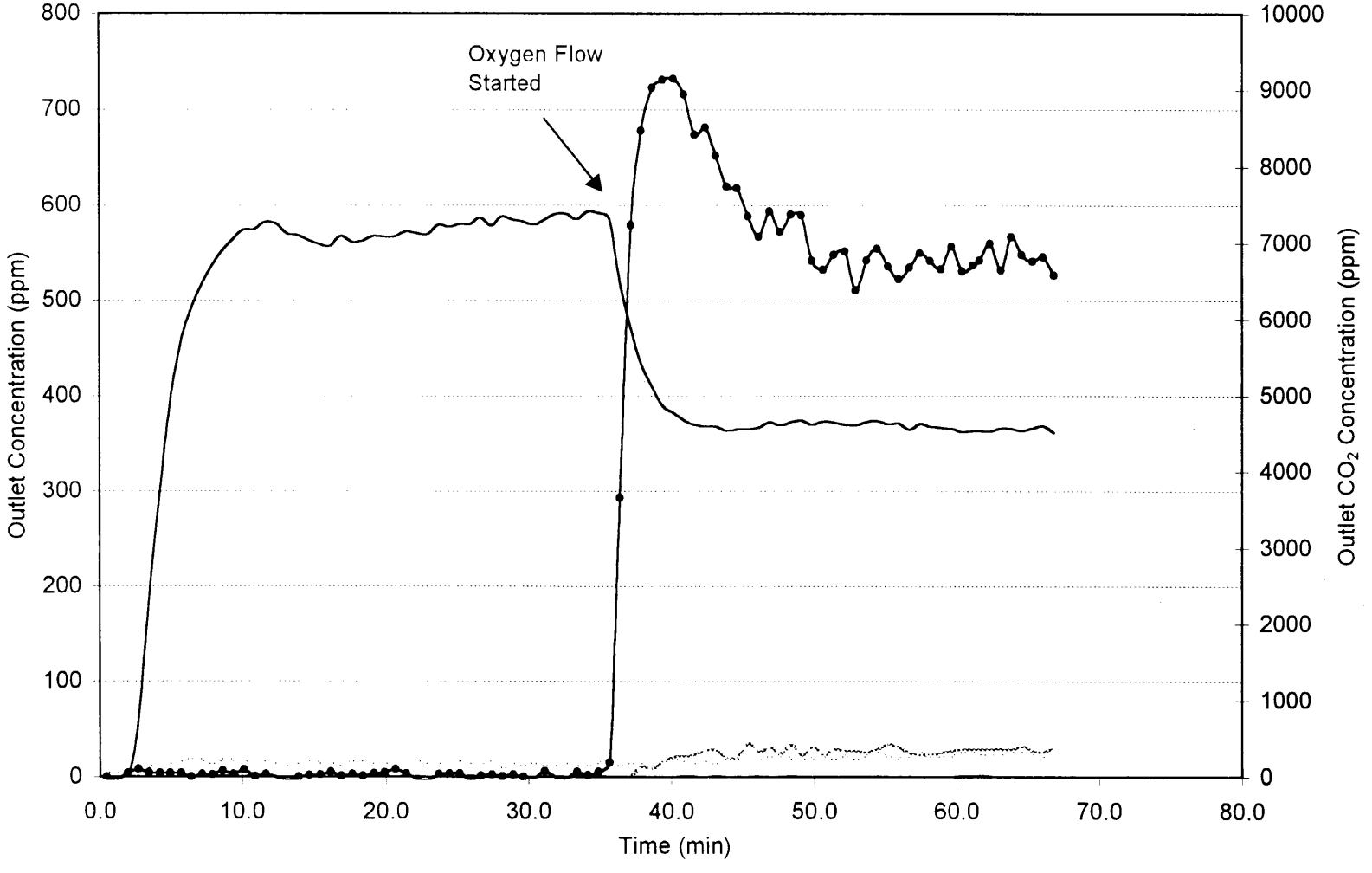

Figure 3.4 Reduction of NO with GAC over PdO/Al_2O_3 Catalyst, GHSV=24,000 [NO]=596 ppm, O_2=5%, Initial Temperature=450°C

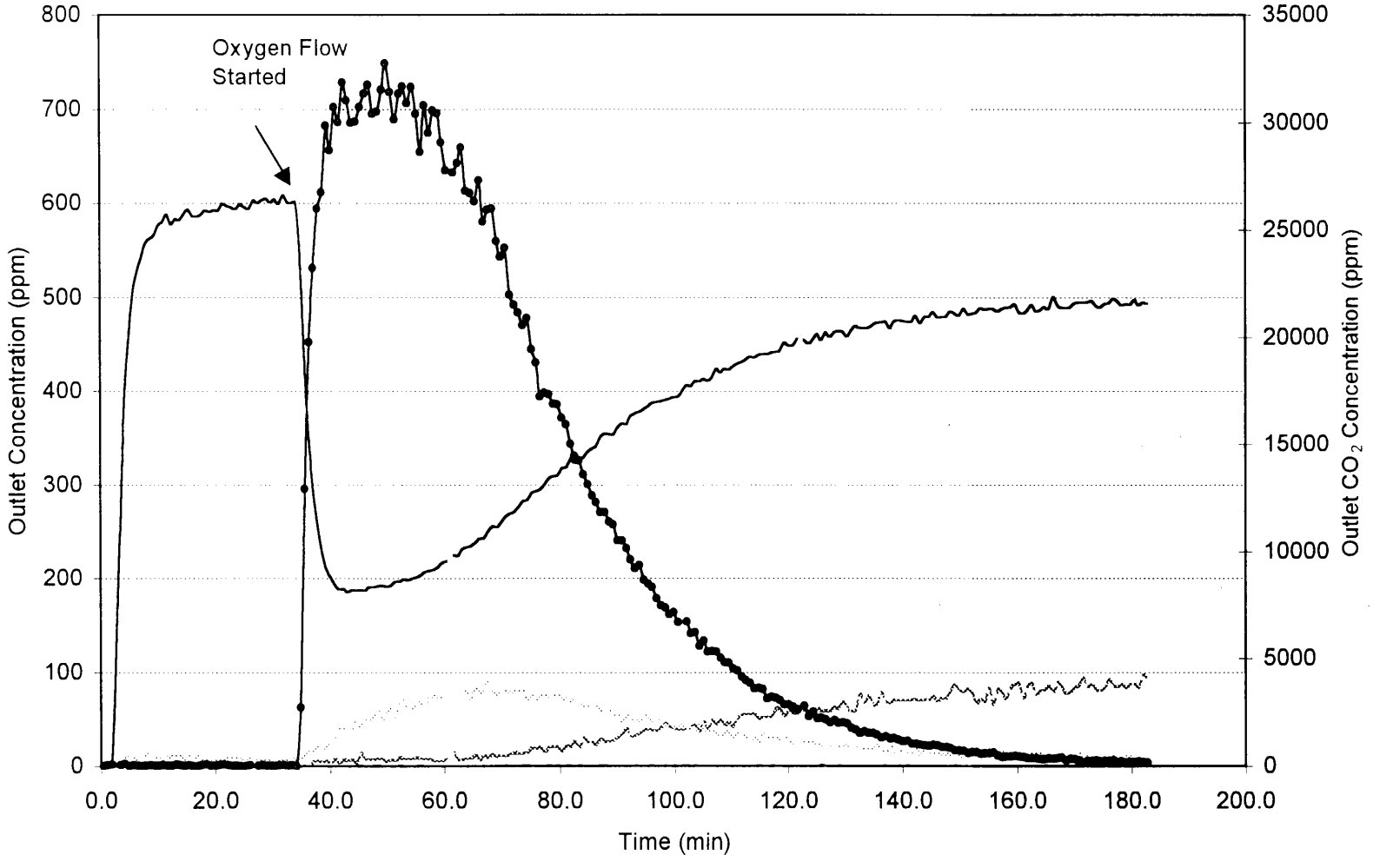

Figure 3.5 Reduction of NO with GAC over PdO/Al_2O_3 Catalyst, GHSV=24,000 [NO]=596 ppm, O_2=5%, Initial Temperature=500°C

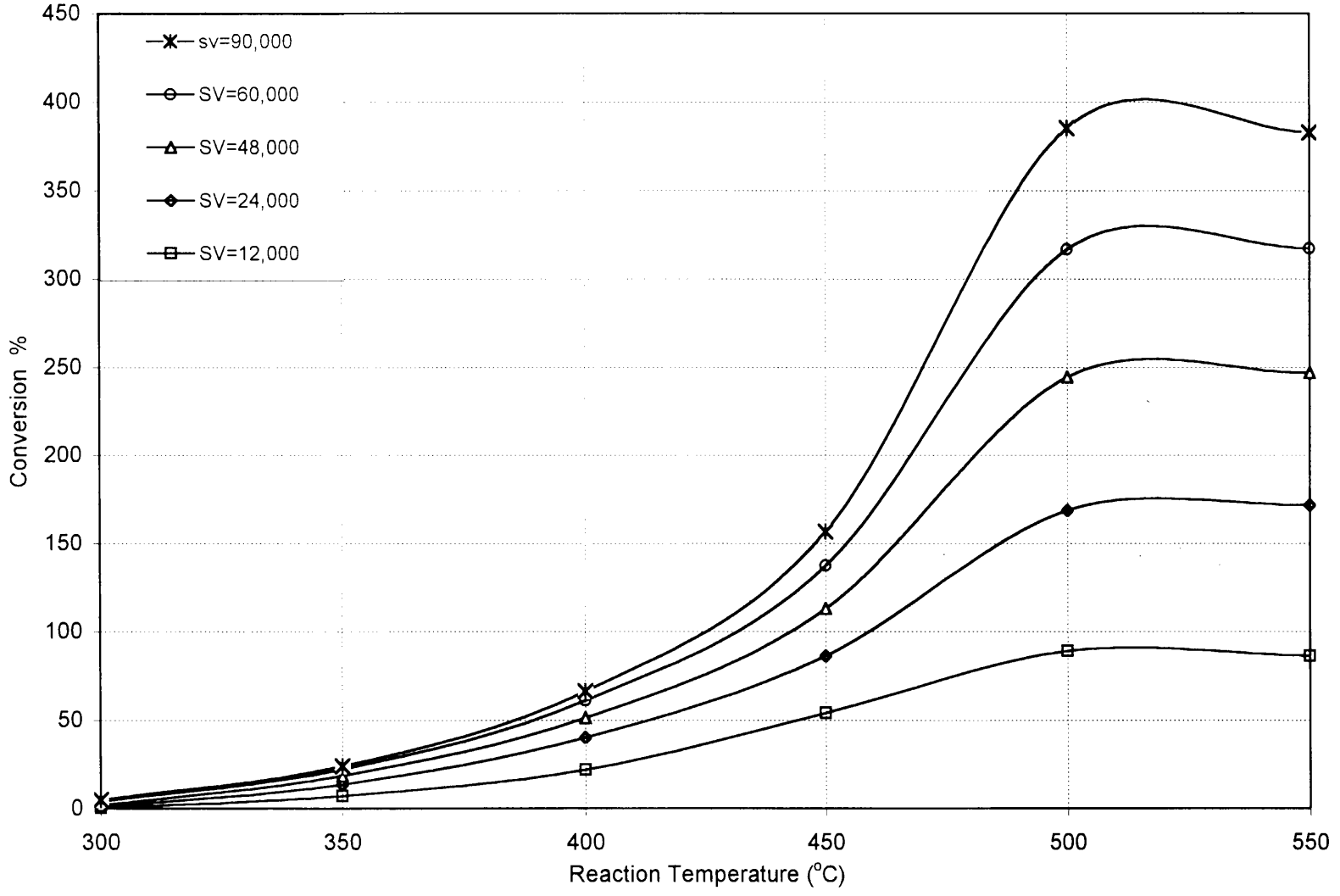

Figure 3.6 Effect of Space Velocity on Reduction of NO with GAC over PdO/Al_2O_3 Catalyst, [NO]=590ppm, $[O_2]$=10%

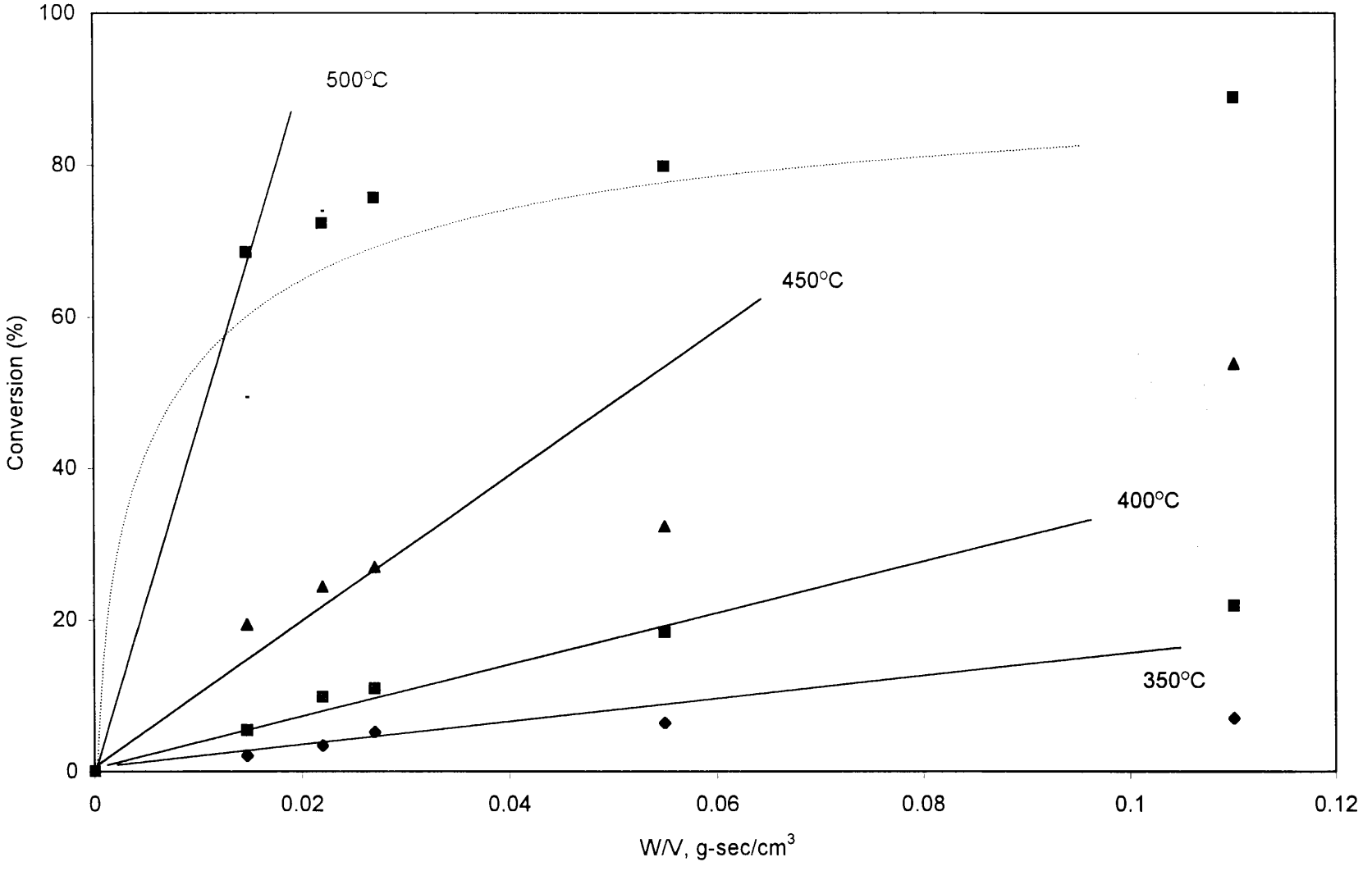

Figure 3.7 Initial Slope for Kinetic Calculation for the NO-O_2-GAC Reactions at 350,400,450,500°C

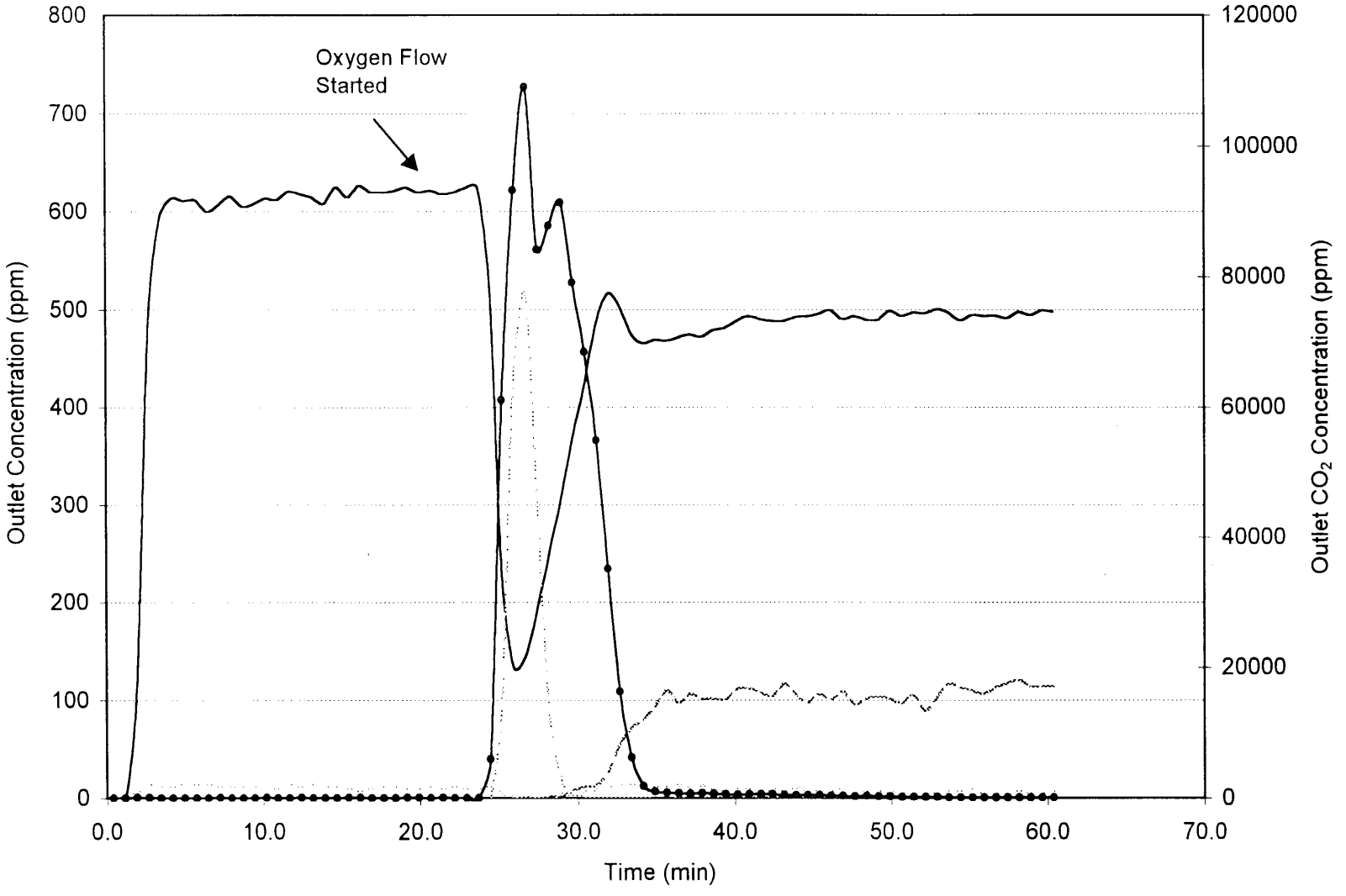

Figure 3.8 Reduction of NO with GAC over PdO/Al_2O_3 Catalyst, GHSV=60,000, [NO]=590ppm, [O_2]=10%, GAC, Initial Temperature =500°C

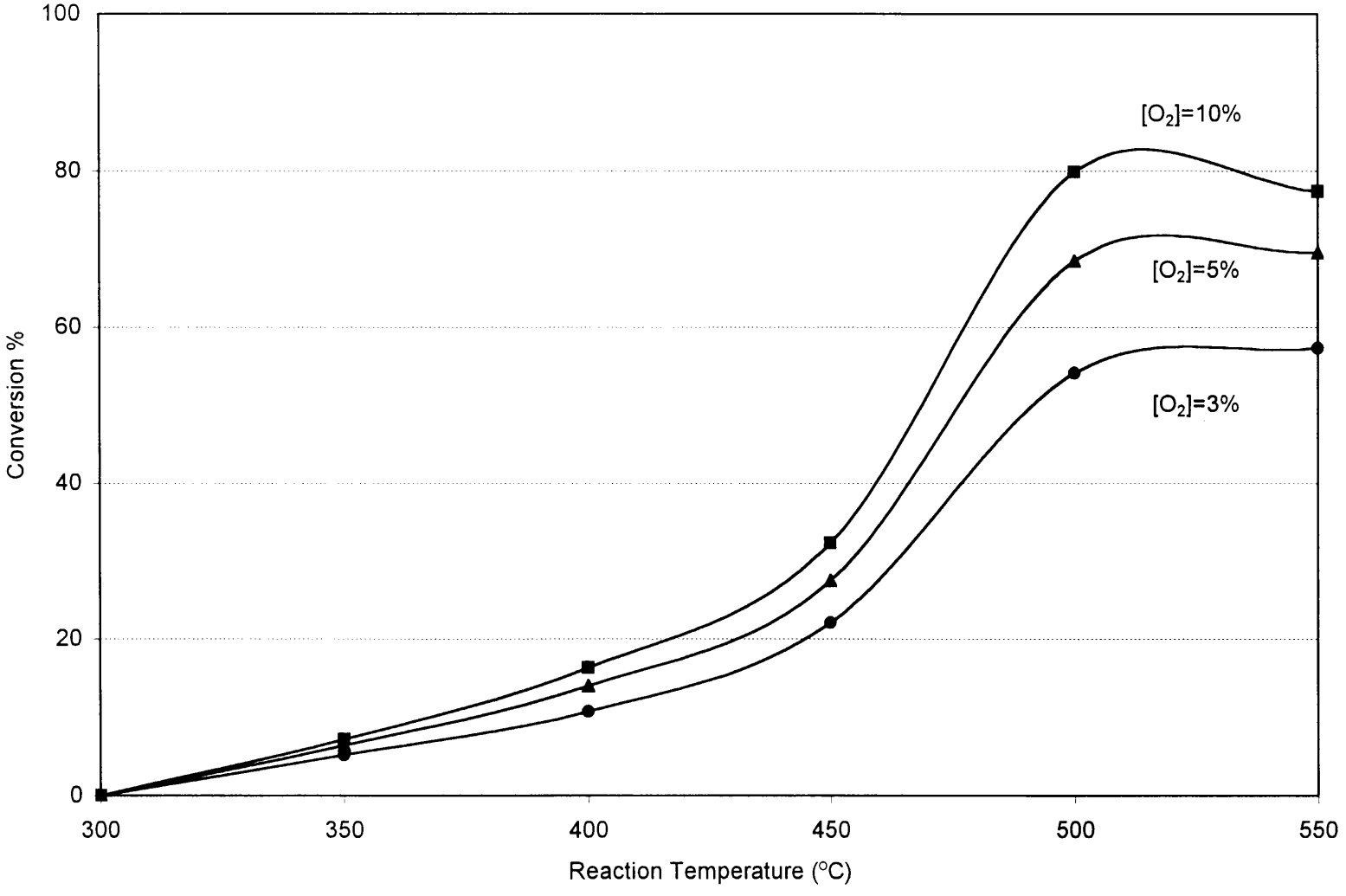

Figure 3.9 Effect of Oxygen Concentration on Reduction of NO with GAC over PdO/Al_2O_3, GHSV=24,000, [NO]=590 ppm

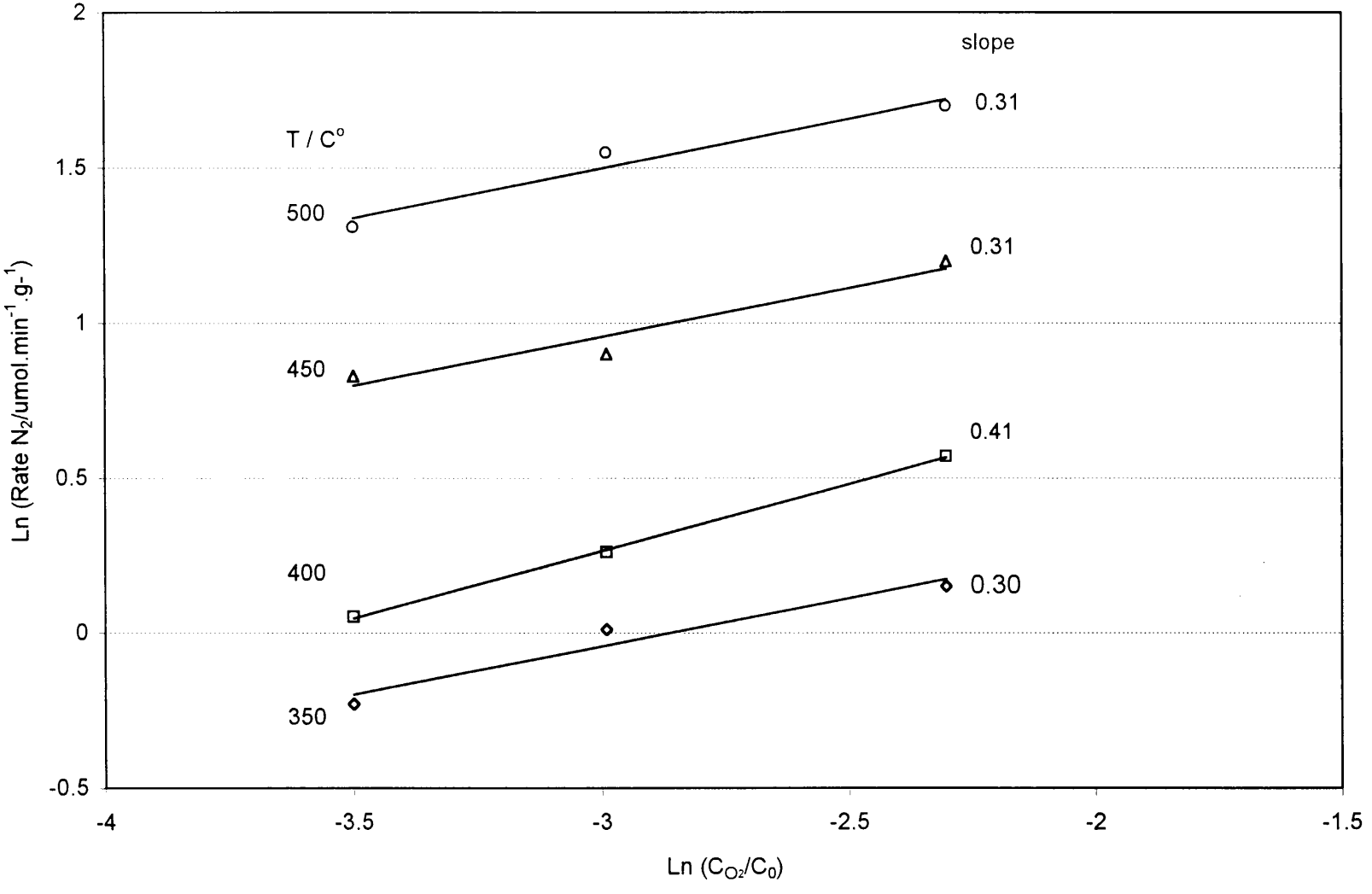

Figure 3.10 The ln-ln Plot Between the Rate of N_2 Formation and the Partial Pressure of O_2 in GAC-NO-O_2 Reaction over PdO/Al_2O_3 Catalyst

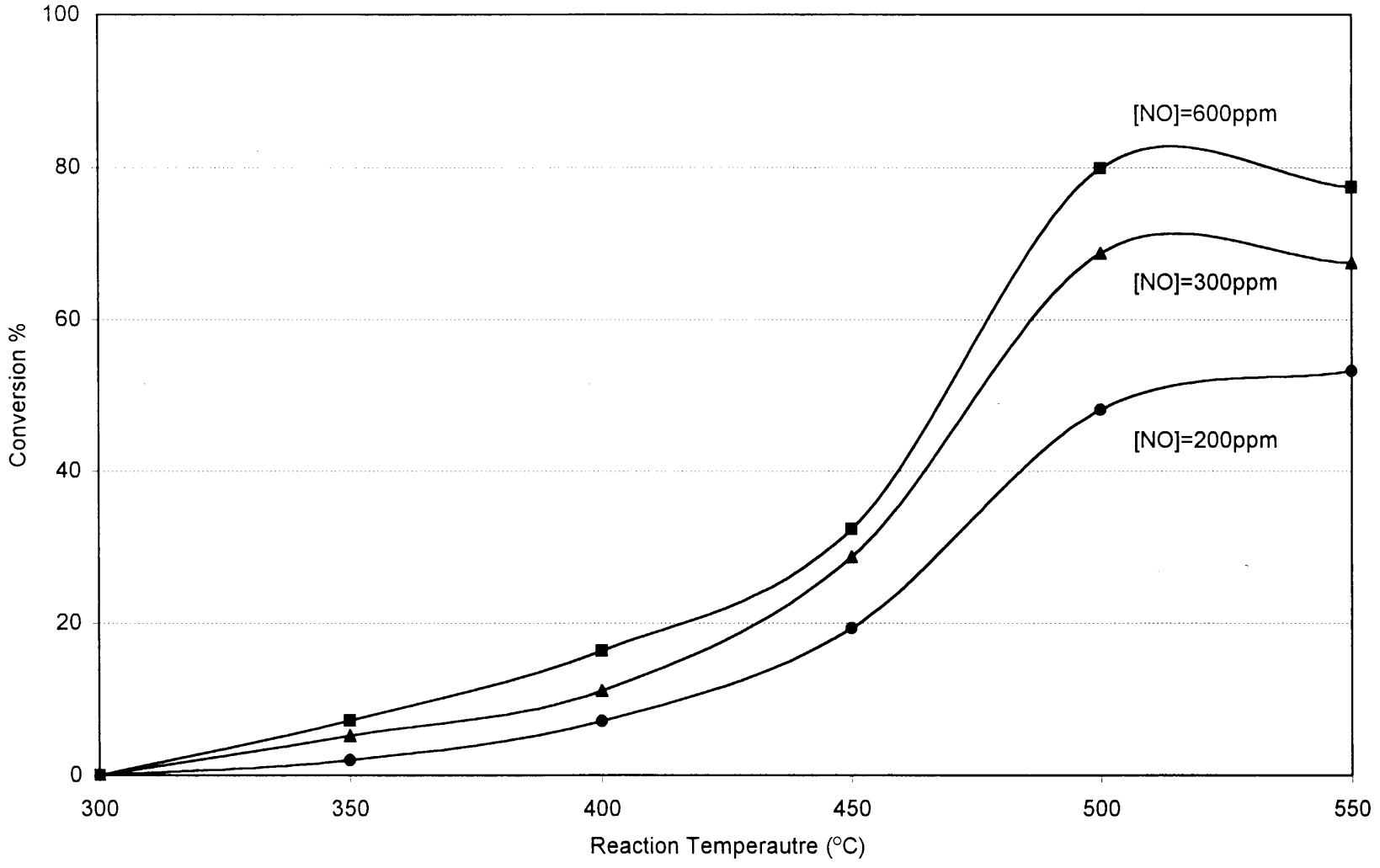

Figure 3.11 Effect of NO Concentration on Reduction of NO with GAC over PdO/Al_2O_3, GHSV=24,000, $[O_2]$=10%

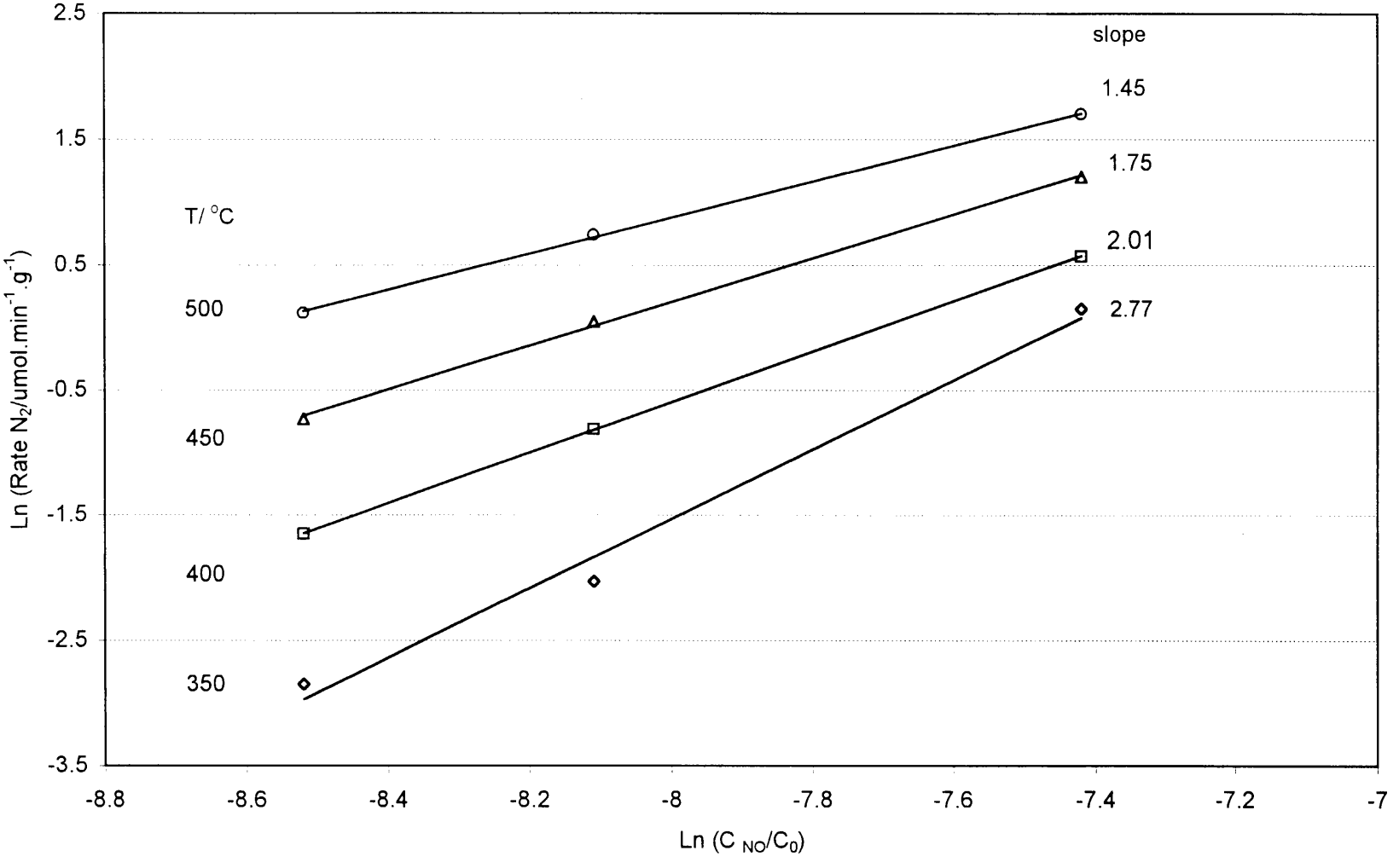

Figure 3.12 The ln-ln Plot Between the Rate of N_2 Formation and the Partial Pressure of NO in GAC-NO-O_2 Reaction over PdO/Al_2O_3 Catalyst

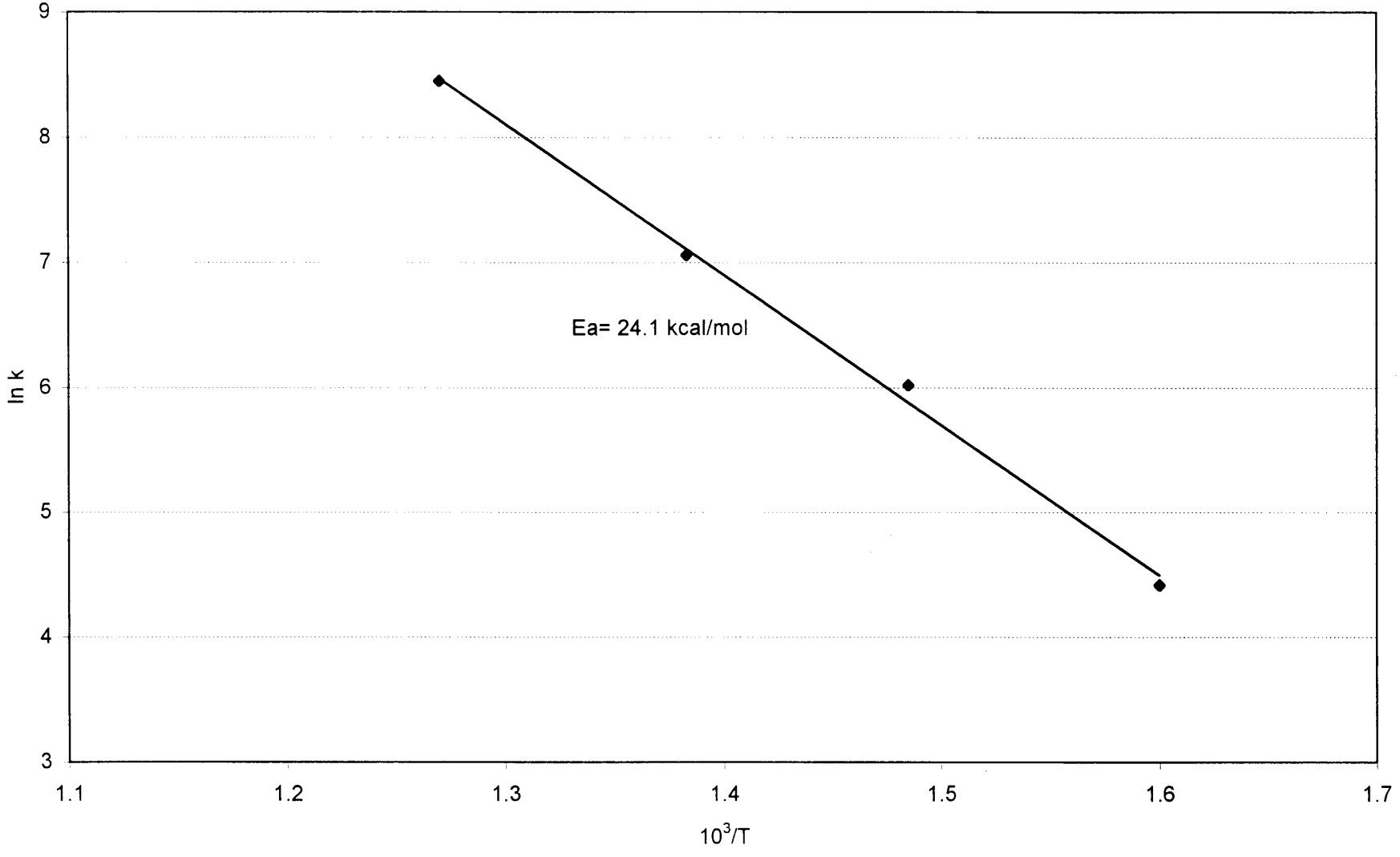

Figure 3.13 Arrhenuis Plot of NOx Reduction with GAC over PdO/Al_2O_3 Catalyst

REFERENCES

1. R. J. Farrauto, Kenneth E. Voss, Rnoald M. Heck, U. S. Patent 5,462,907,

2. R. M. Hecks and R. J. Farrauto, *Catalytic Air Pollution Control*, Van Nostrand Reinhold

3. Held, W. Konig and T. Richter, "Catalytic NOx Reduction in Net Oxidizing exhaust Gas," SAE International Congress and Exposition, Detriot, Michigan, February, 1990

4. M. J. Illan-Gomez, A. Linares, C. Salinas and R. Radovic, "NO Reduction by Activated Carbon," *Energy & Fuels*, Vol. 9, No. 1, 1995

5. M. Iwamoto, H. Yu-u and S. Shundo, *Catalysis Review* 32 (1990) p.430

6. M. Iwamoto, H. Yahiro, S. Shundo, *Appl. Catal.* 69(1991) L15

7. J. Jochheim, D. Hesse, T. Duesterdiek, W. Engeler, D. Neyer, J. P. Warren, A. J. Wikkins, M. V. Twigg, SAE Paper, 962024, 1996

8. F. C. Liu, *Basic Toxicology*, Hemisphere Publishing Corp. 1996

9. K. Matsuoka, H. Orikasa and A. Tomita, " Reaction of NO with Soot over Pt-loaded Catalyst in the Presence of Oxygen," *Applied Catalysis B: Environmental* 26 (2000) pp.89-99

10. J. P. A. Neeft, M. Makkee and J. A. Moulijn, *Appl. Cat.* B 8 (1996) p.57

11. V. Parvulescu, P. Grange and B. Delmon, "Catalytic Removal of NO," *Catalysis Today* 46 (1998) pp.233-316

12. W. F. Shangguan, Y. Teraoka and S. Kagawa, "Kinetics of Soot-O_2, Soot-NO and Soot-O_2-NO Reactions over Spinel-type $CuFe_2O_4$ Catalyst," *Applied Catalysis B: Environmental* 12 (1997) pp.237-247

13. W. F. Shangguan, Y. Teraoka and S. Kagawa, "Simultaneous Catalytic Removal of NOx and Diesel Soot Particulates over Ternary AB_2O_4 Spinel-typ Oxides," *Applied Catalysis B: Environmental* 8 (1996) pp.217-227

14. T. Suzuki, T. Kyotain and A. Tomita, I&EC Res. 33 (1993) p.2840

15. H. Teng, E. M. Suuberg and J. M. Calo, "Studies on the Reduction of Nitric Oxide by Carbon: the NO-Carbon Gasification Reaction," Energy & Fuel 6:398-506, 1992

16. Y. Teraoka and S. Kagawa, "Simultaneous catalytic removal of NOx and diesel soot particulates," *Catalysis Surveys from Japan* 2 (1998) pp.155-164

17. S. Xiao, Kaiwen Ma, Henry Shaw, Robert Pfeffer, John G. Stevens, AIChE Annual Meeting Paper 62z, 1998

18. S. Xiao, K. Ma, X. Tang, I. Bagyi, H. Shaw, R. Pfeffer and J. G. Stevens, " The Lean Catalytic Reduction of Nitric Oxide by Solid Carbonaceous Materials," *Applied Catalysis: B Environmental*, in Press, 2001

19. H. Yamashita and A. Tomita, " Influence of Char Surface Chemistry on the Reduction of Nitric Oxide with Chars," *Energy & Fuels* 1993, 7, 85-89 K.

20. Yoshida, S. Sumiya and R. Helfrich, SAE Paper (1989) 892046